AD-A062 688 CALSPAN ADVANCED TECHNOLOGY CENTER BUFFALO NY F/G 20/4
A STUDY OF INLET CONDITIONS FOR THREE-DIMENSIONAL TRANSONIC COM--ETC(U)
JUN 78 W J RAE, J A LORDI N00019-77-C-0363
UNCLASSIFIED CALSPAN-XE-6129-A-4 NL

OF
AD
A062888

END
DATE
FILMED
3-79
DDC

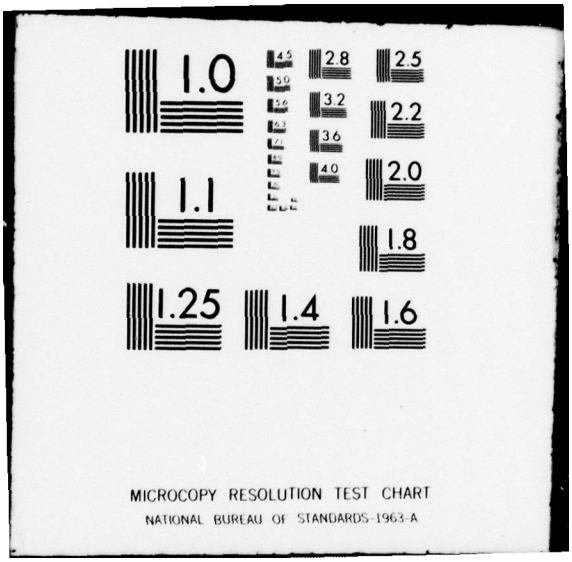
1.0
1.1
1.25
1.4
1.6
1.8
2.0
2.2
2.5
2.8
3.2
3.6
4.0
MICROCOPY RESOLUTION TEST CHART
NATIONAL BUREAU OF STANDARDS-1963-A

NAVAIR

LEVEL II

12

AD A062688

DDC FILE COPY

A STUDY OF INLET CONDITIONS FOR THREE-DIMENSIONAL TRANSONIC COMPRESSOR FLOWS

William J. Rae and John A. Lordi
Calspan Corporation
P.O. Box 400
Buffalo, New York 14225

CALSPAN-XE-6129-A-4

June 1978

66 p.

Final Report for Period 1 June 1977 - 31 May 1978
Contract No. N00019-77-C-0363

Prepared For:

NAVAL AIR SYSTEMS COMMAND
DEPARTMENT OF THE NAVY
WASHINGTON, DC 20361

78 12 22 026

410 803

UNCLASSIFIED

SECURITY CLASSIFICATION OF THIS PAGE *(When Data Entered)*

REPORT DOCUMENTATION PAGE		READ INSTRUCTIONS BEFORE COMPLETING FORM
1. REPORT NUMBER NAVAIR	2. GOVT ACCESSION NO.	3. RECIPIENT'S CATALOG NUMBER
4. TITLE *(and Subtitle)* A STUDY OF INLET CONDITIONS FOR THREE-DIMENSIONAL TRANSONIC COMPRESSOR FLOWS		5. TYPE OF REPORT & PERIOD COVERED FINAL 1 June 1977 - 31 May 1978
		6. PERFORMING ORG. REPORT NUMBER XE-6129-A-4
7. AUTHOR(s) William J. Rae and John A. Lordi		8. CONTRACT OR GRANT NUMBER(s) N00019-77-C-0363
9. PERFORMING ORGANIZATION NAME AND ADDRESS CALSPAN CORPORATION ADVANCED TECHNOLOGY CENTER P. O. BOX 400, BUFFALO, NEW YORK 14225		10. PROGRAM ELEMENT, PROJECT, TASK AREA & WORK UNIT NUMBERS
11. CONTROLLING OFFICE NAME AND ADDRESS NAVAL AIR SYSTEMS COMMAND (AIR-310) DEPARTMENT OF THE NAVY WASHINGTON, DC 20361		12. REPORT DATE June 1978 13. NUMBER OF PAGES 66
14. MONITORING AGENCY NAME & ADDRESS*(if different from Controlling Office)*		15. SECURITY CLASS. *(of this report)* UNCLASSIFIED 15a. DECLASSIFICATION/DOWNGRADING SCHEDULE

16. DISTRIBUTION STATEMENT *(of this Report)*

APPROVED FOR PUBLIC RELEASE:
DISTRIBUTION UNLIMITED

17. DISTRIBUTION STATEMENT *(of the abstract entered in Block 20, if different from Report)*

18. SUPPLEMENTARY NOTES

19. KEY WORDS *(Continue on reverse side if necessary and identify by block number)*

TURBOMACHINERY
COMPRESSORS
TRANSONIC FLOW

20. ABSTRACT *(Continue on reverse side if necessary and identify by block number)*

This report contains a study of the conditions at the inlet of a transonic compressor, with special reference to the formulation of these conditions in a manner suitable for flowfield computation. Several candidate methods for specifying the inlet conditions are reviewed, and details are given for a procedure that uses a matching between finite-difference results and linear-theory formulas at a plane upstream of the rotor.

DD FORM 1 JAN 73 1473 EDITION OF 1 NOV 65 IS OBSOLETE

UNCLASSIFIED

TABLE OF CONTENTS

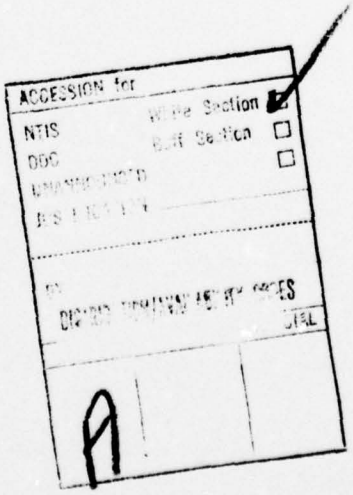

LIST OF FIGURES

LIST OF SYMBOLS

a_∞	speed of sound far upstream
B	number of blades
C_a	axial projection of the chord
$h(s)$	camber line shape
K, L, N	indices numbering the grid points in the z , ζ , ρ directions
L_T	$2\pi r_T / B$
M_∞	u_∞ / a_∞
$\eta(s)$	blade shape
p	pressure
r, θ, X	cylindrical coordinates
s, n	streamwise and normal coordinates in a surface at constant radius
$t(s)$	blade thickness shape
u, v, w	perturbation velocity components in the z , ρ , θ directions
u_n, u_s	perturbation velocity components in the streamwise and normal directions, in a constant-radius surface
u_∞	axial flow speed far upstream
W_z, W_r, W_θ	components of the relative velocity seen by a blade-fixed observer
W_a	$(u_\infty^2 + \omega^2 r^2)^{1/2}$
z	$\omega x / u_\infty$
γ	specific-heat ratio
$\Delta\phi(\rho)$	jump in potential across the trailing vortex sheet
ζ	$\theta - z$
ρ	$\omega r / u_\infty$

LIST OF SYMBOLS (Contd.)

ρ_∞	density far upstream
φ, ϕ	dimensional, non-dimensional velocity potential, respectively
ω	angular velocity of the approach flow, seen by a blade-fixed observer. Also used to denote a relaxation factor.
$()_{H,T}$	denote evaluation at the hub, tip
$()_{u,L}$	denotes evaluation on the upper, lower surface of a blade

Section 1
INTRODUCTION

Axial-flow compressors are used in many aircraft gas-turbine propulsion systems. Improvements in the performance of these devices have always been an important goal of research and development activities, and this goal has taken on new significance in recent years, with increasing demand for maximum thrust with minimum noise and fuel consumption.

The desire for improved performance has led to higher rotational speeds, which produce large regions of transonic flow, where the resultant of the axial inlet velocity of the gas and the angular velocity of the blades exceeds the speed of sound. Thus all of the nonlinear complications of transonic flow are added to a flow pattern that is already quite complex: even when the entire flow is subsonic, it is unsteady and three-dimensional in general, and is strongly influenced by boundary layers on fixed and moving walls, by distortions of the inlet flow, and by a variety of three-dimensional effects. All of these complications are compounded by the introduction of transonic effects, which are typified by large lateral zones of influence and by the presence of shock waves. Thus the flow in a transonic compressor is influenced by some of the most complex phenomena in fluid mechanics.

The extent of these complications together with the great technological importance of axial-flow devices has motivated a great deal of research, and important new advances have been made in recent years, especially in regard to the three-dimensional and transonic features of the flow.[1] These advances include contributions from both experiment[2-5] and theory.[6-25] On the experimental

---

[1] Adamson, T.C. and Platzer, M.F., eds. Transonic Flow Problems in Turbomachinery Hemisphere Publishing Corp., Washington (1977)

[2] Benser, W.A. Bailey, E.E. and Gelder, T.F. "Holographic Studies of Shock Waves Within Transonic Fan Rotors" Paper presented at the ASME Nineteenth International Gas Turbine Conference, Zurich, Switzerland; available as NASA TM X-71430 (30 March-4 April 1974)

[3] Wisler, D.C. "Shock Wave and Flow Velocity Measurements in a High Speed Fan Rotor Using the Laser Velocimeter" ASME Paper 76-GT-49 (March 1976)

side, a variety of non-intrusive measurement techniques have been used to probe the three-dimensional structure of the flow.[2-5] In the area of theoretical advances, a wide variety of computational techniques suited to transonic-flow calculations has been developed.[6-25]

The research described in this report belongs to the latter category. Specifically, it deals with the question of how to specify properly the conditions at the inlet of a transonic compressor. An observer riding on one of the rotor blades of a transonic compressor sees a helical relative approach flow, formed as the resultant of the axial inlet velocity of the gas and the angular velocity of the blades. This inlet relative velocity is typically supersonic at spanwise stations near the tip, and subsonic near the hub. A series of shock waves is generated by the tip sections, while none are produced near the hub; somewhere between these stations a transition must take

---

[4] Gallus, H.E., Bohn, D. and Broichhausen, K.D. "Measurements of Quasi-Steady and Unsteady Flow Effects in a Supersonic Compressor Stage" ASME Paper 77-GT-13 (March 1977)

[5] Dunker, R.J., Strinning, P.E. and Weyer, H.B. "Experimental Study of the Flow Field Within a Transonic Axial Compressor Rotor by Laser Velocimetry and Comparison with Through-Flow Calculations" ASME Paper 77-GT-28 (March 1977)

[6] Alzner, E. Erdos, J. "Unsteady Flow Through Compressor Stages" Advanced Technology Labs., Inc. Report TR-168 NASA CR-127765 (December 1971)

[7] McDonald, P.W. "The Computation of Transonic Flow Through Two-Dimensional Gas Turbine Cascades" American Society of Mechanical Engineers, Paper 71-GT-89 (1971)

[8] Gopalakrishnan, S. and Bozzola, R. "Computation of Shocked Flows in Compressor Cascades" American Society of Mechanical Engineers, Paper 72-GT-31 (1972)

[9] Kurzrock, J.W. and Novick, A.S. "Transonic Flow Around Rotor Blade Elements" Transactions of the ASME Vol. 97 (December 1975) pp. 598-607

[10] Erdos, J., Alzner, E. and McNally, W.D. "Numerical Solution of Periodic Transonic Flow Through a Fan Stage" AIAA Journal 15 No. 11 (November 1977) 1559-1568

[11] Dodge, P.R. "A Transonic Relaxation Method for Cascade Flow Systems" von Karman Institude for Fluid Dynamics, Lecture Series on Transonic Flow in Turbomachinery (May 1973)

place from a flow that is essentially supersonic in character, to one that is subsonic in character. These general physical features of the flow are clearly shown by the laser dual-focus measurements:[5] at a station upstream of the blades, a periodic shock-wave pattern is seen propagating forward* from the outboard stations, while the upstream flow at the inboard stations is composed of disturbances which decay rapidly, in a manner typical of subsonic flow. Any attempt to model these flow features numerically must make allowance for both kinds of behavior, at the upstream boundary of the finite-difference grid. Moreover, this allowance must be made in such a way that the upstream flow at a given spanwise location is dependent on the flow at all other spanwise locations. It is a feature of three-dimensional flows that, even though the velocity is locally supersonic, nevertheless the radial communication that is present leads to an interaction with the subsonic flows farther inboard. It is no longer adequate to use a two-dimensional approximation, in which the upstream wave pattern is uniquely determined by conditions at the given spanwise location.

---

[12] Shope, F.L. and Lakshminarayna, B. "Relaxation Solution of High Subsonic Cascade Flows and Extension of This Method to Transonic Cascades" AIAA Paper 75-23 (January 1975)

[13] Luu, T.S. and Coulmy, G. "Relaxation Solution for the Transonic Flow Through a Cascade" Symposium Transsonicum II, edited by K. Oswatitsch and D. Rues, Springer-Verlag, Berlin, 1976, pp. 331-339

[14] Dodge, P.R. "A Non-Orthogonal Transonic Relaxation Method for Cascade Flows" ASME Paper 76-GT-63, (March 1976)

[15] Ives, D.C. and Liutermoza, J.F. "Analysis of Transonic Cascade Flow Using Conformal Mapping and Relaxation Techniques" AIAA Journal 15 No. 5 (May 1977) 647-652

[16] Sator, F.G. "Computation of Transonic Flow with Detached Bow Shocks Through Two-Dimensional Turbomachinery Cascades" International Council of Aerospace Sciences, Paper 76-40 (October 1976)

[17] Sator, F.G. "Inverse Computation of Profile Shapes for Given Transonic Flow Configurations, with and without Detached Bow Shocks in Two-Dimensional Turbomachinery Cascades" ASME Paper 77-GT-33 (March 1977)

[18] Japiske, D. "Review-Progress in Numerical Turbomachinery Analysis" Journal of Fluids Engineering Trans ASME 98I (December 1976) 592-606

---

* The cases studied herein are restricted to subsonic axial flow, for which these waves propagate upstream.

These general considerations are reviewed in Section 2, which deals with the formulation of the problem, with special attention to the new features peculiar to a fully three-dimensional calculation method. Section 3 then gives a brief description of a number of alternative approaches that were considered. Several of these were judged to be worthy of further development, and two of these were studied further. The approach found to have the greater potential of these two, the matching method, is described fully in Section 4. Section 5 contains the conclusions reached, and recommendations for further development.

---

[19] Novak, R.A. and Hearsey, R.M. "A Nearly Three-Dimensional Intrablade Computing System for Turbomachinery - Part I, General Description; Part II - System Details and Additional Examples" ASME Papers 76-FE-19 and 20 (March 1976)

[20] Hirsch, C. and Warzee, G. "An Integrated Quasi-3D Finite Element Calculation Program for Turbomachinery Flows" ASME Paper 78-GT-56 (April 1978)

[21] Oliver, D.A. "Four Issues in the Computation of Transonic Flows in Turbomachinery" pp. 163-165 of Ref. 1

[22] Oliver, D.A. and Sparis, P. "Computational Aspects of the Prediction of Multidimensional Transonic Flows in Turbomachinery" pp. 567-585 of Aerodynamic Analyses Requiring Advanced Computers Part I, NASA SP-347 (1975)

[23] Paris, D.S., Ganz, A.A. and Liutermoza, J.F. "Some Formulation Considerations in 3-D Transonic Flow Computation" pp. 79-94 of Ref. 1

[24] Veuillot, J.P. "Calculation of the Quasi Three-Dimensional Flow in a Turbomachine Blade Row" Journal of Engineering for Power Trans. ASME 99 (A) (January 1977) pp. 53-62

[25] Rae, W.J. "Calculations of Three-Dimensional Transonic Compressor Flowfields by a Relaxation Method" Journal of Energy 1 (1977) 284-296

Section 2
FORMULATION OF THE PROBLEM

In treating a flow as complicated as this one, an approximate description must be found which is detailed enough to retain the essentials of the problem, but simple enough to work with. For the present case, the nonlinear small-disturbance approximation[25,26] is ideally suited: it retains the essential nonlinearity of the problem and the associated wave structure, yet allows fully three-dimensional flows to be calculated in reasonable times. References 25-29 contain a full description of this method, and the computer program used to calculate examples with subsonic inlet relative Mach number at the tip. In this section, this method is reviewed, with special attention to the boundary conditions required at the inlet.

Basic Equations

The rotor is assumed to be working in a uniform inlet flow, and the flow is assumed to be steady in a coordinate system fixed to the blades. The hub and casing form an annulus of constant diameters. Far upstream of the blade row, the flow seen by a blade-fixed observer has an axial velocity u_∞ and angular velocity ωr .

The coordinate system and rotor geometry used are shown in Figure 1, where the dimensionless variables are defined as

---

[26] Rae, W.J. "Nonlinear Small-Disturbance Equations for Three-Dimensional Transonic Flow Through a Compressor Blade Row" AFOSR TR-76-1082 AD-A031234 (August 1976)

[27] Rae, W.J. "Relaxation Solutions for Three-Dimensional Transonic Flow Through a Compressor Blade Row, in the Nonlinear Small-Disturbance Approximation" AFOSR TR-76-1081, AD-A032553 (August 1976)

[28] Rae, W.J. "Computer Program for Relaxation Solutions of the Nonlinear Small-Disturbance Equations for Transonic Flow in an Axial Compressor Blade Row" Calspan Report No. AB-5487-A-3 (April 1978)

[29] Rae, W.J. "Finite-Difference Calculations of Three-Dimensional Transonic Flow Through a Compressor Blade Row, Using the Small-Disturbance Nonlinear Potential Equation" pp. 228-252 of Ref. 1

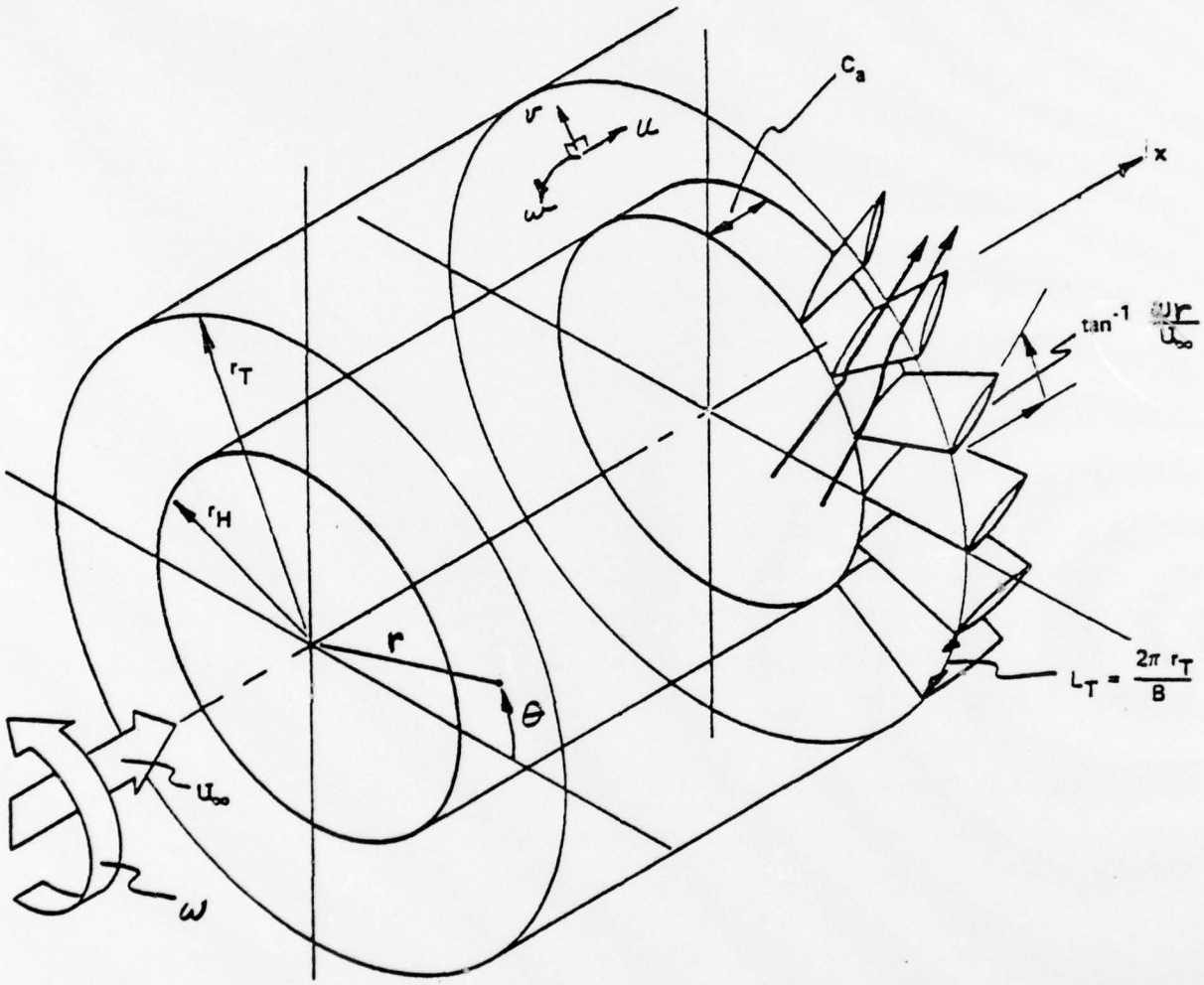

FIGURE 1 BLADE-FIXED COORDINATES
ROTOR IS STATIONARY IN A
HELICAL APPROACH FLOW

$$\bar{z} = \frac{\omega x}{U_\infty} \quad , \quad \rho = \frac{\omega r}{U_\infty} \quad , \quad \zeta = \theta - \bar{z} \quad ; \quad \phi = \frac{\omega \varphi}{U_\infty^2} \tag{1}$$

The velocity components seen by a blade-fixed observer are

$$W_x = U_\infty + u \quad , \quad W_r = v \quad , \quad W_\theta = \omega r + w \tag{2}$$

These dimensional perturbation velocities are related to the velocity potential by

$$\begin{aligned}
\bar{u} &= \frac{u}{U_\infty} = \frac{\partial \phi}{\partial \bar{z}}\Big)_{\rho,\theta} = \frac{\partial \phi}{\partial \bar{z}}\Big)_{\rho,\zeta} - \frac{\partial \phi}{\partial \zeta}\Big)_{\bar{z},\rho} \; ; \\
\bar{v} &= \frac{v}{U_\infty} = \frac{\partial \phi}{\partial \rho}\Big)_{\bar{z},\theta} = \frac{\partial \phi}{\partial \rho}\Big)_{\bar{z},\zeta} \\
\bar{w} &= \frac{w}{U_\infty} = \frac{1}{\rho}\frac{\partial \phi}{\partial \theta}\Big)_{\bar{z},\rho} = \frac{1}{\rho}\frac{\partial \phi}{\partial \zeta}\Big)_{\bar{z},\rho}
\end{aligned} \tag{3}$$

The velocity potential satisfies the equation

$$\begin{aligned}
&\left\{1 - M_\infty^2 (1+\rho^2) - (\gamma+1) M_\infty^2 \phi_{\bar{z}}\right\} \phi_{\bar{z}\bar{z}} + \rho^2 \phi_{\bar{z}\bar{z}} - 2(1+\rho^2)\, \phi_{\zeta\bar{z}} \\
&\qquad + \frac{(1+\rho^2)^2}{\rho^2} \phi_{\zeta\zeta} + (1+\rho^2)\left(\phi_{\rho\rho} + \frac{1}{\rho}\phi_\rho\right) = 0
\end{aligned} \tag{4}$$

Subscripts denote derivatives in the $\bar{z}, \rho, \zeta$ coordinate system; thus the symbol $\phi_{\bar{z}}$ stands for $\frac{\partial \phi}{\partial \bar{z}}\Big)_{\rho,\zeta}$.

This nonlinear equation describes the disturbances caused by the blade row. In a two-dimensional limit, where radial derivatives are zero, it reduces to the transonic small-disturbance equation treated by Murman and Cole.[30] Note that the inlet relative Mach number appears explicitly in the coefficient of the first term:

---

[30] Murman, E.M. and Cole, J.D. "Calculation of Plane Steady Transonic Flows" AIAA Journal 9 pp. 114-121 (1971)

$$M_{rel}^2 = M_\infty^2 (1+\rho^2)$$

There are B blades in the row, and they are taken to lie in the helical surfaces defined by x_∞ and ωr. The axial projection of their chord is a constant, C_a. Thus, they are located at

$$0 \le z \le \frac{\omega C_a}{x_\infty} \; ; \; \rho_H \le \rho \le \rho_T \; ; \; \zeta = \frac{2j\pi}{B} \; , \; j = 0, 1, 2, \ldots, B-1 \qquad (5)$$

If the program is run in the off-design mode, the blade shapes are given by (see Figure 2)

$$\eta_{u_L}(s,r) = h(s,r) \pm \frac{1}{2} t(s,r) - \alpha(r) \cdot s \qquad (6)$$

where h, t and α are the camber, thickness, and angle of incidence. The blade-surface boundary condition is

$$\frac{u_n}{W_o} = \frac{d\eta}{ds} \qquad (7)$$

When the program is run in the design mode, the prescribed quantities are the loading and thickness distributions:

$$\Delta C_p(s,r) \equiv \frac{p_L - p_u}{\frac{1}{2}\rho_\infty x_\infty^2} = -2(1+\rho^2)\left[\left(\frac{u_s}{W_o}\right)_L - \left(\frac{u_s}{W_o}\right)_u\right] \qquad (8)$$

$$t'(s,r) = \frac{d\eta_u}{ds} - \frac{d\eta_L}{ds} \qquad (9)$$

The blade-surface boundary conditions are applied in the helical surfaces $\zeta = 0$ and $\zeta = 2\pi/B$.

Far downstream of the blades, the perturbation potential is expressed as $\phi = Cz$, where

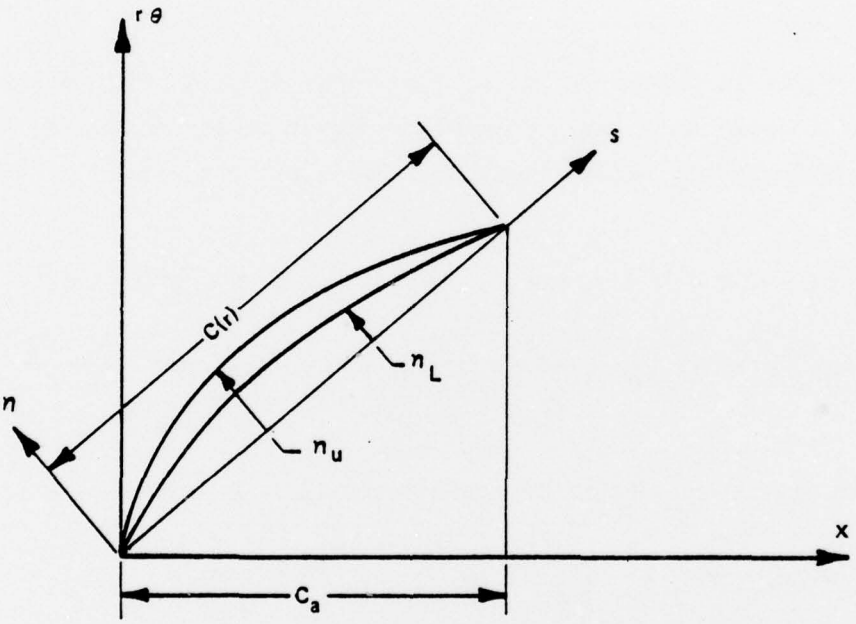

FIGURE 2 DEFINITIONS OF BLADE-SURFACE GEOMETRY

$$C = \frac{-B}{\pi(1-M_\infty^2)(\rho_T^2-\rho_H^2)} \int_{\rho_H}^{\rho_T} \rho \Delta\phi \, d\rho \qquad (10)$$

and where $\Delta\phi(\rho)$ is the spanwise distribution of the circulation. Far upstream of the blades, a radiation condition must be imposed, requiring that any disturbances present shall be traveling in the upstream direction. It is the specific formulation of this condition, suitable for numerical application, that forms the objective of this research.

Numerical Solution

The region in which the solution is to be found is divided into a grid, with the indices L, K and N used to number points in the ζ, z and ρ directions, respectively. Equal spacing is used in the ζ- and ρ-directions:

$$\zeta(L) = (L-1)\Delta\zeta \;,\; L = 1,2,\ldots,LMX \;;\; \Delta\zeta = \frac{2\pi}{B}\Big/(LMX-1) \qquad (11)$$

$$\rho(N) = \rho_H + (N-1)\Delta\rho \;,\; N = 1,2,\ldots,NMX \;;\; \Delta\rho = \frac{\rho_T-\rho_H}{NMX-1} \qquad (12)$$

The spacing in the z-direction is nonuniform; the z-coordinate is taken as

$$z = z(\tau) \quad ; \quad \frac{\partial}{\partial z} = f\frac{\partial}{\partial \tau} \;,\; f \equiv \frac{d\tau}{dz} \qquad (13)$$

The variable τ is then allowed to vary from -1 to +1, as z varies from $-\infty$ to $+\infty$.

$$\tau = -1 + K\Delta\tau \;,\; K = 1,2,\ldots,KMX \;;\; \Delta\tau = \frac{2}{KMX+1} \qquad (14)$$

The particular dependence $z(\tau)$ used here is

$$z(K) = z_M + \frac{1}{2\alpha_1} \ln\frac{1+\tau(K)}{1-\tau(K)} \qquad (15)$$

where

$$z_M = \frac{1}{2}(z_I + z_B)$$

$$z_I = FXI \cdot \frac{\omega C_a}{U_\infty} \quad , \quad z_B = FXB \cdot \frac{\omega C_a}{U_\infty}$$

$$2\alpha_1 = \frac{\ln\left[\Delta\tau/(2-\Delta\tau)\right]}{\frac{1}{2}(z_B - z_I)} \tag{16}$$

The locations of the upstream and downstream edges of the grid are set by the input values for FXB and FXI. Figure 3 shows the general appearance of the grid (with uniform spacing in the z-direction) at constant radius.

The solution of this finite-difference problem has been carried out by a single-line overrelaxation technique. Details of the method were given in Reference 28, and results in Reference 25, for cases where the inlet relative Mach number at the tip was subsonic. For these cases, all disturbances must vanish, far upstream of the blades; this condition was achieved by requiring the perturbation potential to be zero at $K = 1$.

It should be emphasized that the solutions found by this method are "fully three-dimensional", i.e., no further approximations to the radial derivatives are made, beyond those already contained in the differential equation. In this sense, the solution must be distinguished from "quasi three-dimensional" solutions.[19-20] The latter are essentially a set of weakly coupled two-dimensional solutions in neighboring blade-to-blade planes. The degree of coupling varies from one method to another, but never reaches the level of evaluating the radial derivatives at all points. In constrast, the numerical work described above carries the full radial communication throughout the flow. No assumptions peculiar to any given radius are made, and all quantities are free to adjust themselves radially. One of the features observed in the solutions is a radial redistribution of the mass flow, as the streamtubes at various radii adjust their cross-sectional areas in response to the pressure gradients imposed by the blading.[25]

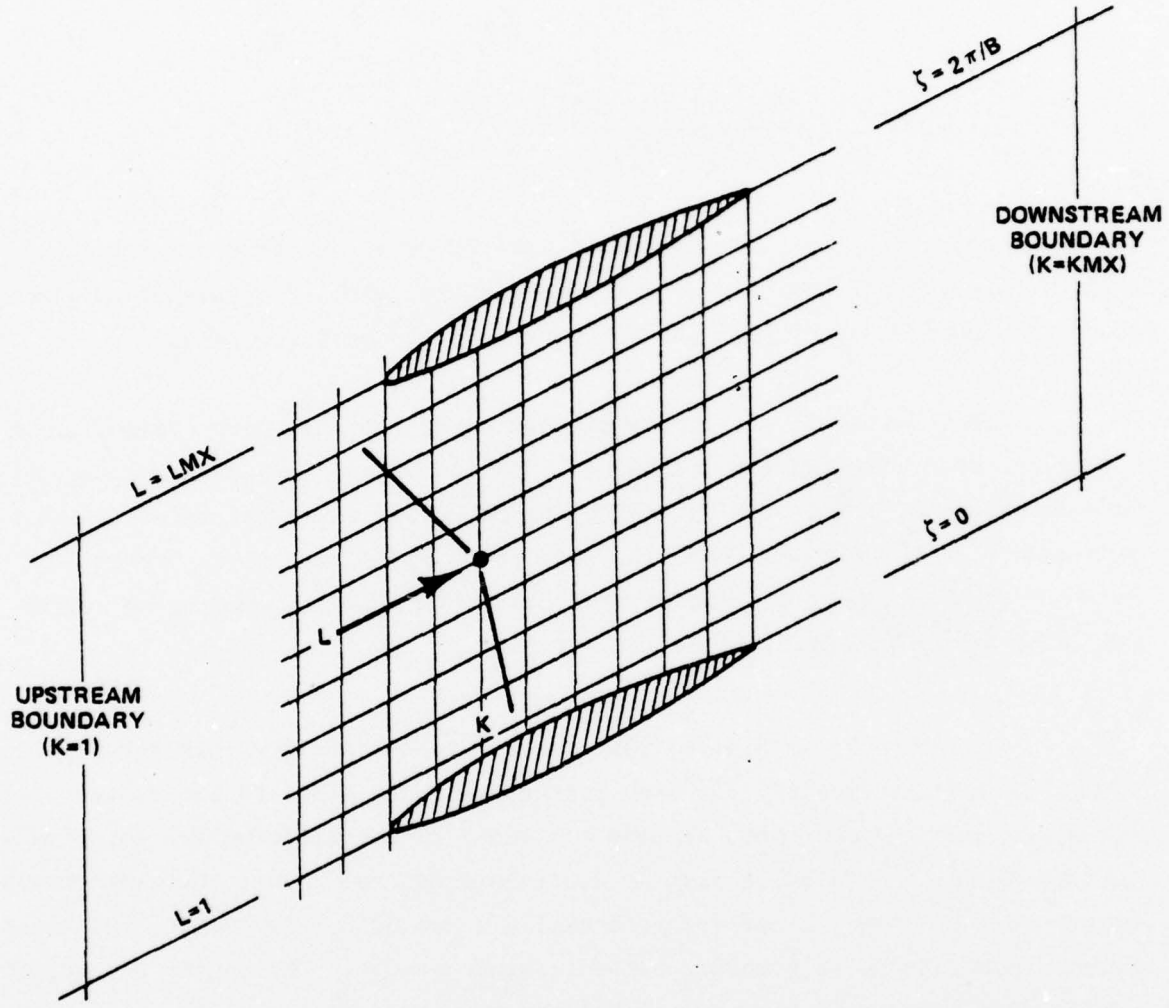

FIGURE 3 COORDINATE SYSTEM AND FINITE-DIFFERENCE GRID, SHOWING FORWARD MACH CONE AT POINT K, L. SURFACE SHOWN IS AT CONSTANT RADIUS (N = CONSTANT)

For the cases of concern here, the condition that disturbances vanish at the upstream grid boundary is not adequate, because it is possible for disturbances of nonzero amplitude to be radiated forward from the blade row. The appropriate condition is then a radiation condition, which states that any wavelike disturbances present in the flow must not have originated upstream of the grid boundary. Figures 4a and 4b illustrate the types of patterns that are envisioned by this condition. In Figure 4a, the shock waves that are generated near the blade leading edges are radiated upstream. Figure 4b is a representation of what might happen if these waves were reflected at a grid boundary. The reflected waves would obviously be an artifact of the finite-difference procedure, and a means must be found for eliminating them.

In the fully linearized approximation (corresponding to $\gamma = -1$ in Equation 4) the radiation condition is easy to apply. In that case, the general solution can be written as a Fourier-Bessel series; the eigenfunctions containing the axial dependence display both families of waves, and the proper set is chosen by setting the appropriate coefficients equal to zero in each term.[31-37] Unfortunately, this term-by-term operation does not suggest any equivalent formula that might achieve the same effect on the sum.

---

[31] McCune, J.E. "The Three-Dimensional Flow Field of an Axial Compressor Blade Row-Subsonic, Transonic, and Supersonic" Ph.D. Thesis Cornell University (February 1958)

[32] McCune, J.E. "A Three-Dimensional Theory of Axial Compressor Blade Rows - Application in Subsonic and Supersonic Flows" Journal of the Aerospace Sciences Vol. 25 No. 9 (September 1959) pp. 544-560

[33] McCune, J.E. "The Transonic Flow Field of an Axial Compressor Blade Row" Journal of the Aerospace Sciences Vol. 25 No. 10 (October 1958) pp. 616-626

[34] Okurounmu, O. and McCune, J.E. "Three-Dimensional Vortex Theory of Axial Compressor Blade Rows at Subsonic and Transonic Speeds" AIAA Journal Vol. 8 No. 7 (July 1970) pp. 1275-1283

[35] Okurounmu, O. and McCune, J.E. "Lifting Surface Theory of Axial Compressor Blade Rows: Part I - Subsonic Compressor; Part II - Transonic Compressor" AIAA Journal 12 (October 1974) pp. 1363-1380

[36] Lordi, J.A. "Report on a Study of Noise Generation by a Rotating Blade Row in an Infinite Annulus" U.S. Air Force Office of Sciencitic Research Report AFOSR TR-71-1485; also available as Calspan Report No. AI-2836-A-1 (May 1971)

[37] Lordi, J.A. "Noise Generation by a Rotating Blade Row in an Infinite Annulus" AIAA Paper No. 71-617 AIAA 4th Fluid and Plasma Dynamics Conference, Palo Alto, California (21-23 June 1971)

a.) WITHOUT REFLECTION

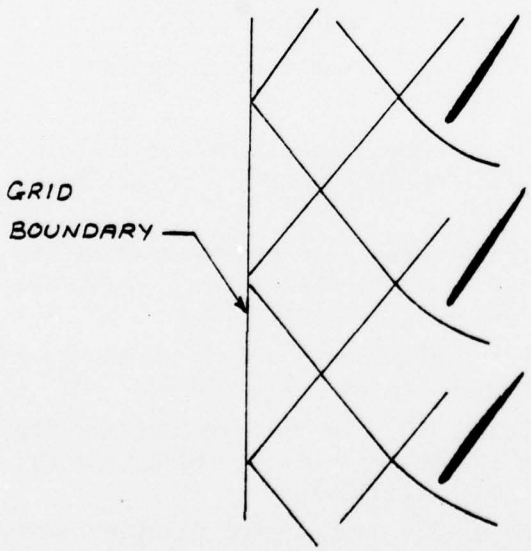

b.) WITH REFLECTION

FIGURE 4 WAVE PATTERNS EXPECTED

Thus, while the radiation condition is easy to describe, it is nevertheless very difficult to formulate, in terms suitable for a numerical calculation. In the next section, a review is given of a number of candidate methods for doing so.

Section 3
REVIEW OF ALTERNATIVE APPROACHES

This section contains a description of some of the formulations of the inlet conditions that have been used in other flowfield calculations, with comments on their suitability for the present problem.

Uniform Flow

The disturbances generated by the blade row diminish in amplitude as they propagate forward. Thus it might be hoped that the imposition of uniform-flow conditions would be an adequate boundary condition, especially if the upstream grid boundary is located sufficiently far from the blades. There are published results of turbomachinery flowfield calculations which have used this procedure.[9,22,38] Thompkins and Epstein point out the inconsistency of this procedure, but note that the acoustic energy being radiated has a small effect on the flow in the vicinity of the rotor.

The approximation chosen for the present study is a more sensitive one, however, in that the rotors are lightly loaded, so that all disturbances are small. An attempt was made to carry out a supersonic-tip-speed calculation, using the computer program described in Reference 28, which employ a uniform flow at $K = 1$. The results showed that stable solutions could not be found; instead, a series of waves travels back and forth between the blades and the grid boundary with an amplitude that decreases in the upstream direction. These wavelike disturbances are located mainly at the outer spanwise stations, where the inlet relative Mach number is supersonic. They also influence the flow in the subsonic regions closer to the hub, but their effect decays very rapidly toward the hub.

These tendencies are displayed in Figures 5-7, which contain results for a blade row having 23 blades, a hub/tip ratio $h = 0.5$, solidity $C_a / L_T = 0.5$ operating with $M_\infty = 0.5$, $M_T = 1.2$, so that the inlet relative Mach number

[38] Thompkins, W.T. and Epstein, A.H. "A Comparison of the Computed and Experimental Three-Dimensional Flow in a Transonic Compressor Rotor" AIAA Paper 76-368 (July 1976)

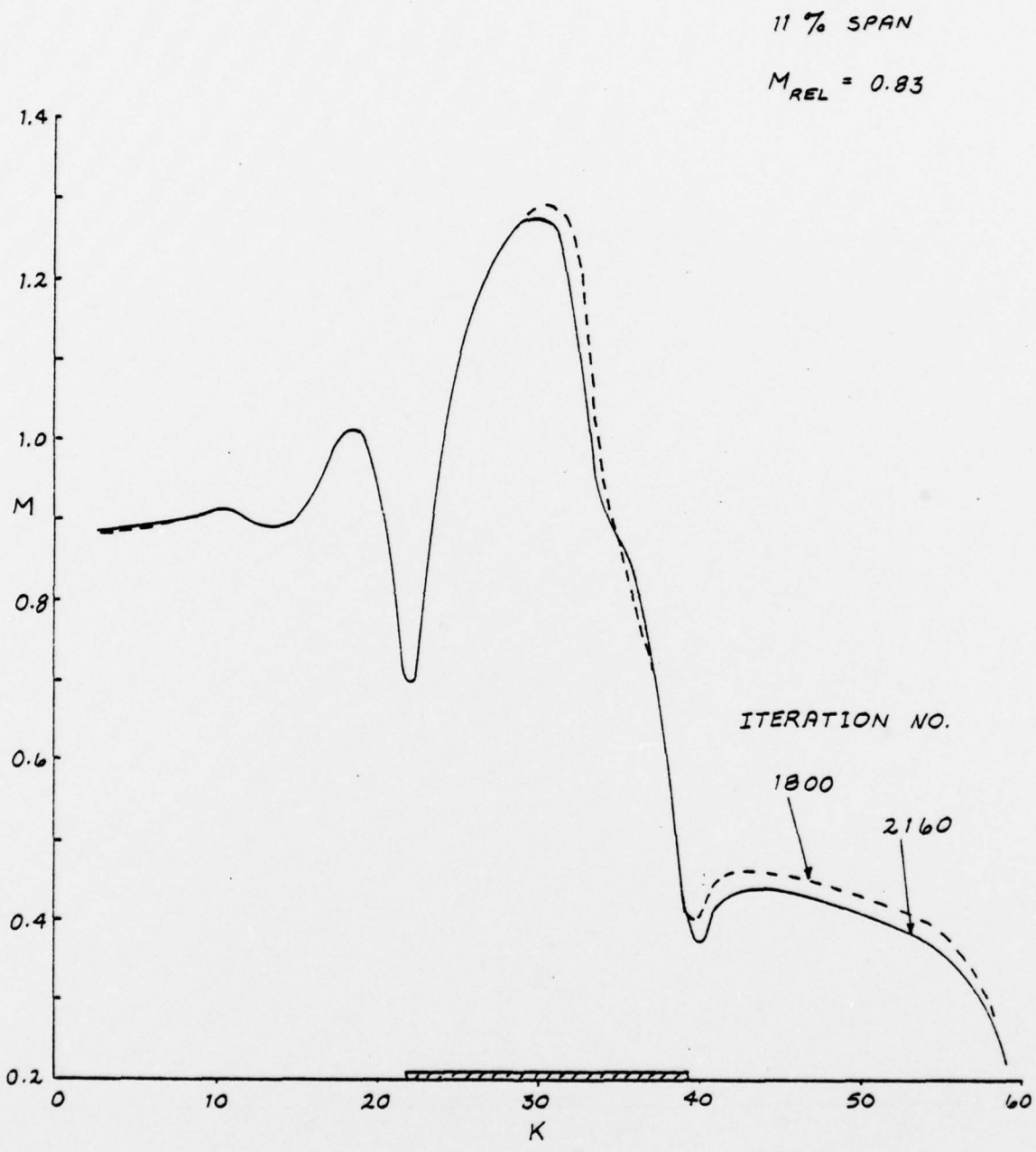

FIGURE 5 MACH-NUMBER DISTRIBUTION, $\zeta = 0$

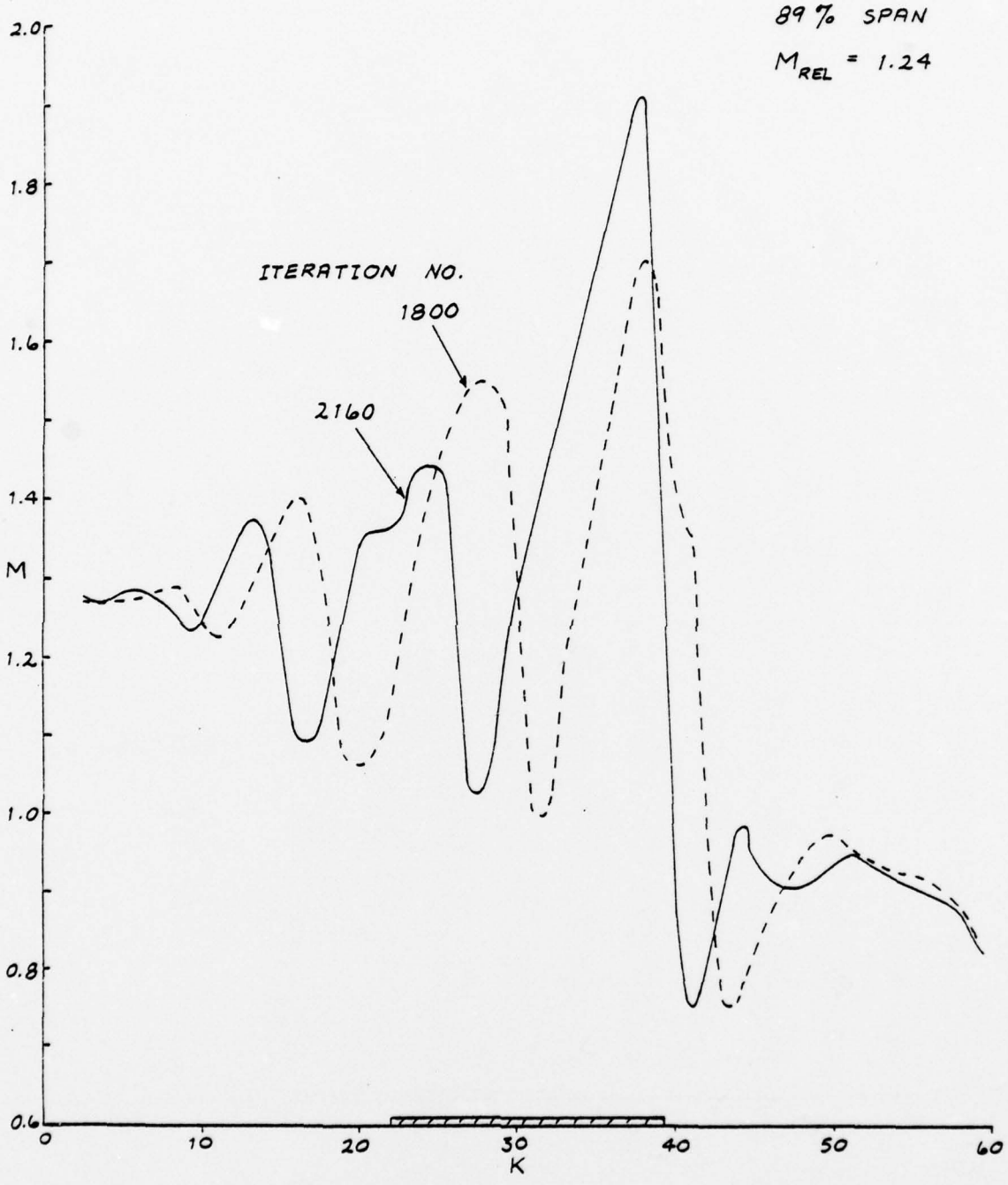

FIGURE 6 MACH-NUMBER DISTRIBUTION, $\zeta = 0$

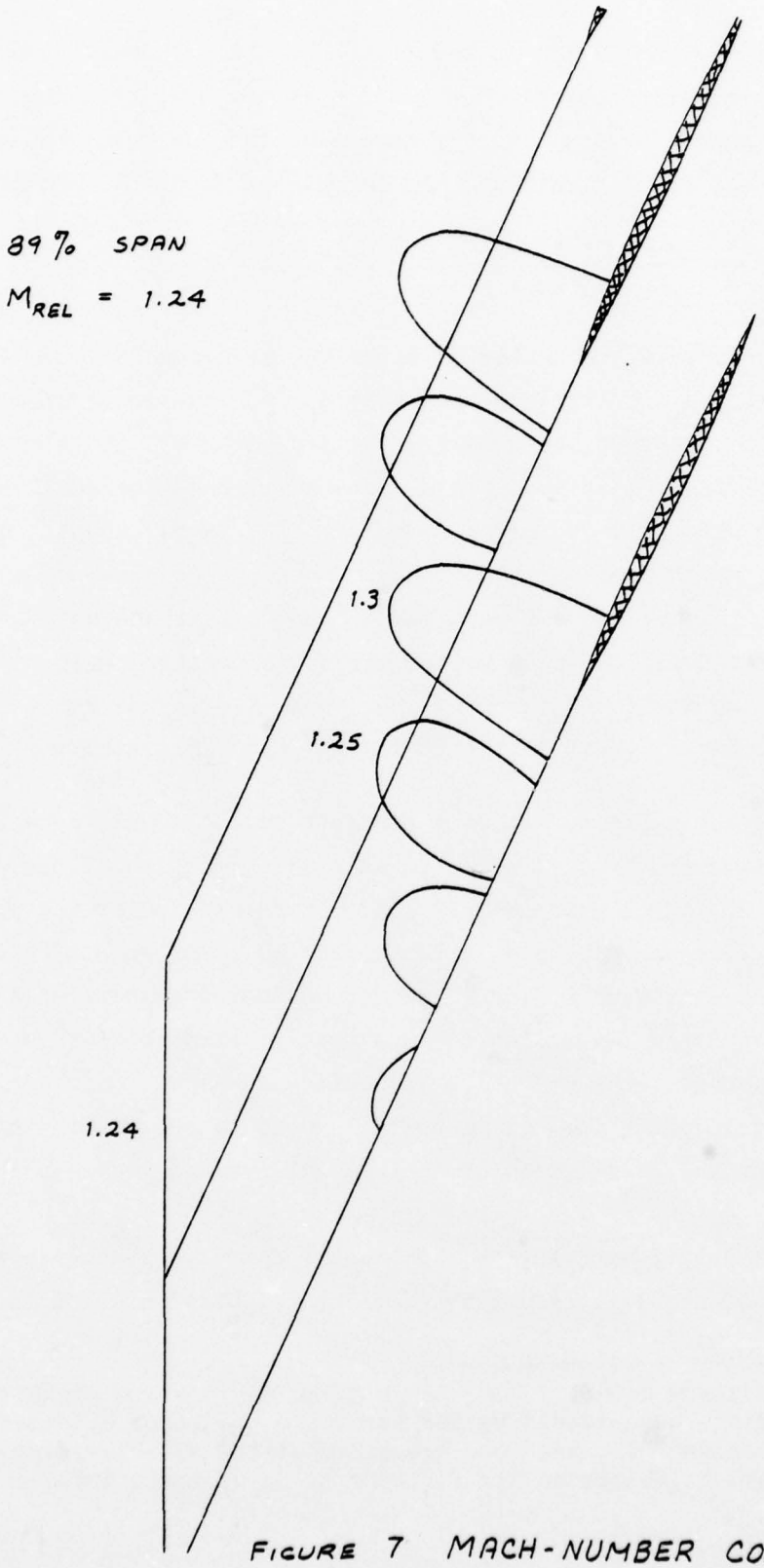

FIGURE 7 MACH-NUMBER CONTOURS

varied from 0.78 at the hub to 1.3 at the tip.* Figure 5 shows the Mach number distribution at an inboard station (ρ = 1.333), at two stages in the iteration process. The Mach number is shown as a function of the index K , which numbers the grid points in the axial direction. It is related to axial location by

$$\frac{x}{C_a} = \frac{1}{2} - \frac{7}{2} \frac{\ln(K/61-K)}{\ln(1/60)} \quad , \quad K = 1, 2, 3, \ldots, 60$$

The iteration number counts the number of times the solution has been updated at the point in question. Numbers on the order of 2000 are large enough for the solution to have converged, for the grid size used here. It is clear that the solution has converged at this inboard station, with only a small response to the changes that are still occurring outboard. The latter changes are illustrated in Figure 6, which pertains to ρ = 2.267. Here the movement of waves is readily evident. Figure 7 shows Mach number contours at the outboard station; one would expect that these contours would open up, and extend upstream at approximately the Mach angle. Apparently, this behavior is prevented by the imposition of the constant level M = 1.24 at the upstream grid boundary.

It is interesting to note that a separate set of calulations was done for precisely the same conditions, but with an earlier version of the computer program (Reference 27) which used a four-point representation of the mixed derivative $\phi_{\zeta z}$. This earlier calculation converged after only 1300 iterations, and showed no evidence of wave motion. However, as noted in Reference 25, calculations done with the four-point formula have great difficulty showing any waves at all. Apparently, the effective viscosity associated with the truncation error of the four-point formula is very large, with the result that all of the waves present in the solution are spread out over many grid points.

The two calculations described above were done for incidence angles on the order of 15 to 20 degrees, resulting (for the calculation using the four-point

---

*Details of the blade-row geometry and operating conditions are given in Appendix A. These calculations were funded by the Air Force Office of Scientific Research and Calspan Corporation IR&D, and were presented at the AFOSR Program Review Meeting, held at Wright-Patterson Air Force Base, 25-26 April 1977.

formula) in stagnation pressure ratios on the order of 1.3. Thus the disturbances generated were quite large - in fact, large enough to strain the limits of applicability of the small-disturbance approximation. Within this approximation, it appears that the factor which determines whether stable solutions can be found is not the relative magnitude of the acoustic and blade-induced disturbances, but rather it is the basic ability of the finite-difference procedure to capture the waves.

Another feature of these calculations that should be noted is that the coordinates were "stretched" in the axial direction. This has the effect of placing the upstream boundary a greater physical distance from the blades, for a given grid size. This is an effective procedure for subsonic inlet cases, where the potential itself is assigned (equal to zero) on the upstream boundary. The stretching used in the cases reported above assigned zero potential values at three chord lengths upstream of the blade row. Thus a substantial advantage was given to the uniform-inlet boundary condition. The fact that it did not yield stable solutions must be taken as evidence that the solution contained substantial variations, even at several chords upstream of the blade row, and the uniform inlet conditions were inconsistent with these variations.

The coordinate-stretching technique loses its advantages when the boundary conditions involve derivatives of the potential (as seems likely to be the case, if wave-induced velocities are to be used). The reason is that finite-difference representations of these derivatives introduce derivatives of the coordinate transformation, which generally become large, at large distances from the blades. Thus, as noted by Magnus (Reference 39), the attempt to assign boundary values at arbitrarily large distances may be defeated by arbitrarily large values of the coordinate-transformation derivatives.

The net conclusion to be drawn is that uniform inlet conditions are not acceptable, although they may lead to converged solutions, especially if the finite-difference method is not sensitive to wavelike structures.

---

[39] Magnus, R.J. "Computational Research on Inviscid, Unsteady, Transonic Flow over Airfoils" Convair Division of General Dynamics Report CASD/LVP 77-010 (January 1977)

Two-Dimensional Approximations

Measurements of the wave pattern near the tip of a transonic compressor (References 5, 40, 41, for example) show structures that are essentially two dimensional, and two-dimensional analyses, usually of the simple-wave variety, have often been used[42-44] to interpret these structures. Thus, it is tempting to use the two-dimensional formulas to assign the flowfield at the upstream grid boundary.

It is clear what formulas would be used at stations where the inlet relative Mach number is greater than one. However, there is no comparable set of formulas for the subsonic stations inboard. It seems reasonable to assume zero disturbances, far enough upstream in the subsonic zone. However, it is not clear what degree of approximation would be introduced by assigning such a uniform subsonic region adjacent to a two-dimensional simple-wave region, even if the singular behavior of the latter at Mach number one could be overcome.

Moreover, the construction described above would give rise to nonzero values of the radial velocity, which might be quite large in the vicinity of the sonic radius. These nonzero values of $\partial\Phi/\partial\rho$ are inconsistent with the two-dimensional assumption that produced them in the first place.

---

[40] Schwenk, F.C., Lewis, G.W. and Hartman, M.J. "A Preliminary Analysis of the Magnitude of Shock Losses in Transonic Compressors" NACA RM E57A30 (March 1957)

[41] Miller, G.R. and Bailey, E.E. "Static-Pressure Contours in the Blade Passage at the Tip of Several High Mach Number Rotors" NASA TM X-2170 (February 1971)

[42] Levine, P. "Two-Dimensional Inflow Conditions for a Supersonic Compressor with Curved Blades" Journal of Applied Mechanics 24 (1957) pp. 165-169

[43] Fink, M.R. "Shock Wave Behavior in Transonic Compressor Noise Generation" Trans ASME 93 (D) Journal of Engineering for Power No. 4 (October 1971) 397-403

[44] Lichtfuss, H.J. and Starken, H. "Supersonic Cascade Flow" pp. 37-149 of Progress in Aerospace Sciences Vol. 15 ed. by D. Kuchemann Pergamon Press, New York (1974)

It may be found eventually that a modified form of the two-dimensional, simple-wave picture is a satisfactory boundary condition, and the agreement with experiment, at least for stations near the tip, requires that this be the case. However, the viewpoint of the research reported here is that quasi-two-dimensional behavior must be a product of the calculations, and not an input to them. For this reason, no attempt has been made to apply the two-dimensional formulas on a strip-theory basis. Instead, the requirement has been set that the boundary condition to be used at the upstream grid boundary must not be specific to each radius, but must encompass all radii simultaneously, and must allow full communication between all radii.

One implication of this three-dimensional communication is that the concept of unique incidence, familiar in two-dimensional approximations,[44] no longer applies. The unique incidence requirement arises from the fact that a supersonic flow can pass through a preassigned area distribution only for a unique value of the mass flow. If the flow is assumed to be two-dimensional, then the blade geometry fixes the area distribution. However, if the flow is three-dimensional, then the stream tubes are free to find their required cross-sectional area by deflecting radially, and it is no longer true that the blade geometry alone determines the allowed incidence.

Relations Used in Unsteady Methods

Many of the methods currently used for turbomachinery flowfield calculations are based on the time-dependent equations of motion.[6-10,21-24] For cases that are expected to be steady in blade-fixed coordinates, the boundary conditions do not vary in time, and the steady state is achieved as the large-time limit of the unsteady solution. In this approach, the basic equations are always hyperbolic, and have real characteristics, which can be used to calculate conditions at the upstream grid boundary.

In the present work, the assumption of steady flow in blade-fixed coordinates is used from the outset to simplify the equations by reducing the number of dependent variables from four to three. One effect of this step is

to yield a mixed (hyperbolic/elliptic) equation which does not have real characteristics in the subsonic regions. In their absence, what is sought is a radiation condition, uniformly applicable to supersonic and subsonic regions.

Although the method-of-characteristics approach of the unsteady methods is not directly applicable, it does, however, suggest a technique that might be useful for the quasi-steady equations used here.

The technique referred to is suggested by the fact that the iteration process used to solve the quasi-steady equations can be thought of as equivalent to an unsteady method, with the iteration count playing the role of time. Indeed, it is precisely this analogy that motivates the selection of terms to be updated on each iteration, following the analysis of Jameson.[45] Thus it is possible to construct an unsteady equivalent of the quasi-steady equation, with time-dependent terms corresponding to the specific choices made for updating various values of the potential. It is possible that one or more of these equivalent unsteady equations might serve as the basis for constructing a radiation condition suited to the iteration process.

In particular, recent studies[46-48] have addressed the question of shock-wave motion in unsteady two-dimensional transonic flows. This motion was calculated by a shock-fitting method, in which the shock-jump equation used, derived from the unsteady potential equation, contains the shock-wave velocity explicitly. It seems reasonable to assume, in general, that the motion of captured shocks in iterative methods probably follows the unsteady shock-jump relations corresponding to the equivalent unsteady equations being used.

---

[45] Jameson, A. "Iterative Solution of Transonic Flows over Airfoils and Wings, Including Flows at Mach 1" Communications on Pure and Applied Mathematics 27 pp. 283-309 (1974)

[46] Yu, N.J., Seebass, A.R. and Ballhaus, W.F. "An Implicit Shock-Fitting Scheme for Unsteady Transonic Flow Computations" AIAA Paper 77-633 (June 1977)

[47] Fung, K.Y., Yu, N.J. and Seebass, A.R. "Small Unsteady Perturbations in Transonic Flows" AIAA Paper 77-675 (June 1977)

[48] Seebass, A.R., Yu, N.J. and Fung, K.Y. "Unsteady Transonic Flow Computations" Paper presented at the AGARD Fluid Dynamics Panel Symposium on Unsteady Aerodynamics, Ottawa, Canada (September 1977)

If this is the case, then it might be possible to tailor the selection of updating rules in such a way as to obtain an equivalent unsteady equation whose wave-motion properties yield outward-moving waves.

The number of research questions posed by this possibility was felt to be so numerous as to place it beyond the scope of the present effort, and no further attention was given to it. However, it may hold enough promise to warrant further consideration in future studies.

Modified Linear Theory

It was noted above that the fully linearized small-disturbance theory can be expressed in closed form, as an infinite sum of eigenfunctions. In each term, the coefficients are chosen in such a way as to enforce the radiation condition. Thus it is natural to turn to these series expressions when searching for a radiation condition applicable to the nonlinear small disturbance theory. The basic idea is to make evaluations of the linearized theory for typical cases, and to learn from these results what structure is introduced by the radiation condition.

One of the complications of this approach is that the solution displays a resonance phenomenon at transonic speeds where some of the eigenfunctions become infinite. The amplitudes of these modes can be kept finite by the introduction of viscous damping[31] or by the addition of a linearized form of the nonlinear term.[35] On the basis of McCune's results,[35] the latter approach was judged to be the preferable one, and a fair amount of attention was given to the derivation of the appropriate formulas, and the development of a computer program for evaluating the eigenfunction solutions for given cases.

Calculations were made for the blade-thickness contribution to the flow field upstream of a typical transonic rotor. In the course of this work, limitations were discovered in the approximate representation of the transonic nonlinearity. The approximation, which amounts to a parabolic method, replaces the streamwise acceleration by a constant. Unless this constant is positive,

the linear acoustic description of the far field cannot be recovered. However, the flow through a compressor rotor is, on the average, decelerating; thus the choice of the constant for a given case is a rather arbitrary procedure.

While results of these calculations can provide some guide to the formulation of a radiation condition, it was felt that the matching method, described below, was a preferable choice. Details of the modified linear theory and the results obtained are presented in Appendix B.

Matching Method

The final approach considered, and the one adopted, was a matching between the linear theory and the numerical solution, at a station upstream of the leading edge. This method is described in detail in the next section.

Section 4
MATCHING METHOD

It is standard practice in transonic flowfield computations to use an analytic representation of the far field. For example, the original calculations by Murman and Cole[30] of the subsonic flow over a nonlifting airfoil used a doublet as the far-field solution. The strength of the doublet was a function of the solution itself, and was updated as the solution progressed.

An analogous procedure is applicable to the present problem; at sufficient distance upstream of the rotor, the disturbances can be expected to have decreased to a level that can be described by the linear theory. The linear theory, in turn, does contain the required radiation condition, albeit in an obscure fashion. Thus an exact solution of the problem, in principle, is to use the finite-difference method for a portion of the flowfield and the linear theory for the remainder, matching the two solutions at some suitable station:

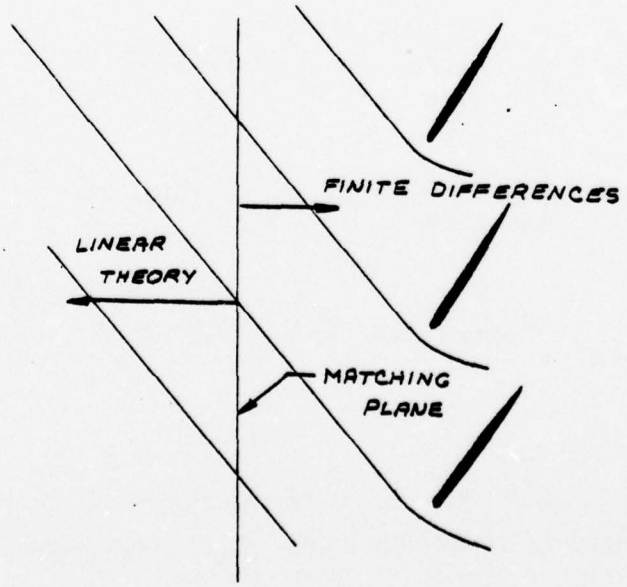

The reason for labeling the linear-theory radiation condition as "obscure" is that the linear solution is written as a Fourier-Bessel series of eigenfunctions. In each of the terms of this series, the radiation condition is easy to apply by choosing the branch of the axial wavenumber in such a way as to correspond to outward-moving waves. However, it is not clear that any simple condition, applied to the sum of all the modes, would give the same results as the term-by-term treatment.

Because this approach is in principle exact, it was selected as the main focus of the research reported here. The principal task addressed was to look for ways of simplifying the calculations. In what follows, the derivation of the Fourier-Bessel series is reviewed first; following that, the procedures used in evaluating the coefficients in the series are described. Lastly, the results found from application to a specific case are given.

Fourier-Bessel Series

The linearized form of Equation 4 has the following Fourier-Bessel series solution:[31-37]

$$\phi(\bar{z},\rho,\zeta) = A_{oo} + \sum_{k=1}^{\infty} A_{ok}\, e^{\lambda_{ok}(\bar{z}-\bar{z}_u)}\, R_{ok}(K_{ok}\sigma)$$

$$+ 2\times R.P.\left\{ \sum_{m=1}^{\infty} \left[\sum_{k=1}^{k^*} A_{m\beta k} R_{m\beta k}(K_{m\beta k}\sigma)\, e^{im\beta\zeta}\, e^{i\left[\frac{m\beta}{\beta^2}+\mu_{m\beta k}\right](\bar{z}-\bar{z}_u)} \right.\right.$$

$$\left.\left. + \sum_{k=k^*+1}^{\infty} A_{m\beta k} R_{m\beta k}(K_{m\beta k}\sigma)\, e^{im\beta\zeta}\, e^{i\frac{m\beta}{\beta^2}(\bar{z}-\bar{z}_u)}\, e^{\lambda_{m\beta k}(\bar{z}-\bar{z}_u)} \right] \right\} \tag{17}$$

where $\sigma = \rho/\rho_T$, $\beta^2 = 1 - M_\infty^2$, B is the number of blades, $\bar{z}_u$ is the station at which the matching is to be done, and $R_{m\beta k}$ is a normalized combination of Bessel functions:

$$R_{m\beta k}(K_{m\beta k}\sigma) = Z_{m\beta k}(K_{m\beta k}\sigma) / N_{m\beta k}$$

$$Z_{m\beta k}(K_{m\beta k}\sigma) = J_{m\beta}(K_{m\beta k}\sigma) - \frac{J'_{m\beta}(K_{m\beta k})}{Y'_{m\beta}(K_{m\beta k})} Y_{m\beta}(K_{m\beta k}\sigma) \tag{18}$$

Here J_n and Y_n are the Bessel functions of the first and second kinds, of order n, and the normalization factor $N_{m\beta k}$ is

$$N^2_{m\beta k} = \frac{1}{2}\left\{\left[1 - \left(\frac{m\beta}{K_{m\beta k}}\right)^2\right] Z^2_{m\beta k}(K_{m\beta k}) - \left[h^2 - \left(\frac{m\beta}{K_{m\beta k}}\right)^2\right] Z^2_{m\beta k}(K_{m\beta k} h)\right\} \tag{19}$$

The normalization is such that

$$\int_h^1 \sigma R_{nk}(K_{nk}\sigma) R_{n\ell}(K_{n\ell}\sigma)\, d\sigma = \begin{cases} 1, & \ell = k \\ 0, & \ell \neq k \end{cases} \tag{20}$$

where the quantity h is the hub/tip radius ratio ρ_H / ρ_T, and the $K_{m\beta k}$ are the eigenvalues satisfying the boundary condition of no flow through the wall, which reduces, for an annulus of constant diameters, to

$$\frac{J'_{m\beta}(K_{m\beta k})}{Y'_{m\beta}(K_{m\beta k})} = \frac{J'_{m\beta}(K_{m\beta k} h)}{Y'_{m\beta}(K_{m\beta k} h)} \tag{21}$$

Procedures for the numerical determination of these eigenvalues are described in Reference 36, with special attention to the case where both the order and the argument of the Bessel functions are large. The quantities λ and μ are given by:

$$\mu_{m\beta k} = \frac{m\beta}{\beta^2 \rho_T}\left\{M_T^2 - \beta^2\left(\frac{K_{m\beta k}}{m\beta}\right)^2\right\}^{1/2} = -i\lambda_{m\beta k}, \quad m \neq 0 \tag{22}$$

$$\lambda_{ok} = \frac{K_{ok}}{\beta \rho_T} \tag{23}$$

The index k^* identifies the modes which are "cut off", i.e., for $k > k^*$, the mode is damped (because $\lambda > 0$, $z < z_u$).

In a complete linear theory, the amplitude coefficients A_{mBk} must be related to the blade geometry and loading. For the present case, however, they are chosen so as to match the calculated values of the potential at the station $z = z_u$. The sequence used is as follows: the finite-difference calculation is started [using the computer code described in Reference 28] as though the inlet relative Mach number at the tip were subsonic, i.e., the condition $\phi = 0$ is applied at the upstream edge of the grid ($K=1$). This upstream boundary is placed at several chord lengths upstream of the leading edge. The solution is allowed to run for a number of iterations in the axial and radial directions. At this point, the iterations are interrupted, and the values of ϕ at a station KA (typically one chord upstream of the leading edge) are fitted by the Fourier-Bessel series, i.e., the coefficients A_{mBk} are chosen so as to match the numerical data at the station KA . The iterations are then resumed, at stations $K \geq KA$. On the upstream side of KA , however, the potential distribution is held at the values found from the fitted series. In particular, some of the velocity components ϕ_z that enter the nonlinear term at supersonic points are calculated by differencing the fitted ϕ values.

The fitting procedure can be repeated at preassigned intervals in the iteration process. The objective is to find a practical location and frequency for the fitting procedure such that wavelike disturbances originating at the blades are not sent back into the flowfield as reflected waves.

Evaluation of the Coefficients

The general formula used for the A_{mBk}'s is found, by using the orthogonality relation (Eq. 20), as:

$$A_{mk} = \frac{B}{2\pi} \int_0^{2\pi/B} \int_h^1 \phi(\sigma, \zeta, \bar{z}_u) e^{-imB\zeta} R_{mBk}(K_{mBk}\sigma)\, \sigma\, d\sigma\, d\zeta \tag{24}$$

The data to be fitted are specified at a set of discrete points in the σ, ζ plane. In the computer program, these points are identified by the indices L, N where

$$\zeta(L) = (L-1)\,\Delta\zeta \quad , \qquad L = 1, 2, \ldots, LMX$$

$$\sigma(N) = \frac{1}{\rho_T}\left\{\rho_H + (N-1)\,\Delta\rho\right\}, \quad N = 1, 2, \ldots, NMX$$

In order to carry out the integrals, a linear interpolation of the data is used; as a result, each of the A_{mk}'s can be written as a weighted sum of the values of ϕ being fitted, where the weights are independent of the fitted data, as follows:

$$A_{mk)_{\substack{real\\imag}}} = \frac{B}{2\pi} \int_h^1 R_{mBk}(K_{mBk}\sigma)\, \sigma\, \mathcal{I}(\sigma)\, d\sigma \tag{25}$$

where

$$\mathcal{I}(\sigma)_{\substack{real\\imag}} = \int_0^{2\pi/B} \begin{matrix}\cos\\ -\sin\end{matrix} (mB\zeta)\ \phi(\sigma, \zeta\,;\, \bar{z}_u)\, d\zeta$$

$$= \sum_{L=2}^{LMX} \int_{\zeta(L-1)}^{\zeta(L)} \begin{matrix}\cos\\ -\sin\end{matrix} (mB\zeta) \left\{\frac{\zeta - \zeta(L-1)}{\Delta\zeta}\,\phi(L) - \frac{\zeta - \zeta(L)}{\Delta\zeta}\,\phi(L-1)\right\} d\zeta \tag{26}$$

where $\phi(L)$ stands for $\phi(\sigma, \zeta(L)\,;\, \bar{z}_u)$. This sum is then written in the form

$$\mathcal{I}(\sigma)_{\substack{real\\imag}} = \sum_{L=1}^{LMX} WT(L, m)_{\substack{real\\imag}}\ \phi(L, KA, N) \tag{27}$$

where KA and N define $\bar{z}_u$ and σ, respectively. The weights WT are straightforward integrals of the sine and cosine, multiplied by 1 or ζ.

After the integral $\mathcal{I}(\sigma)$ is determined, the coefficients A_{mk} can be found, again by a linear interpolation, as follows:

$$A_{mk} = \frac{B}{2\pi} \sum_{N=2}^{NMX} \int_{\sigma(N-1)}^{\sigma(N)} \sigma R_{mBk}(K_{mBk}\sigma) \left\{ \frac{\sigma - \sigma(N-1)}{\Delta\sigma} \mathcal{I}(N) - \frac{\sigma - \sigma(N)}{\Delta\sigma} \mathcal{I}(N-1) \right\} d\sigma$$

$$\equiv \sum_{N=1}^{NMX} U(N) \mathcal{I}(N) \qquad (28)$$

where the weights $U(N)$ are integrals of powers of σ times the function R_{mBk}. These integrals were done by Simpson's rule.

The computer program described in Reference 28 was augmented by an appropriate set of subroutines which calculate the weighting factors WT and U. These calculations are done at the beginning of the calculation, and are stored for later use. The station KA at which the fitting is to be done is selected by an input value. The fitting is done at intervals in either the axial or radial iterations; these intervals are also set by input values, called ITKRAD and ITRRAD, respectively.

The term A_{oo} would not be included if one were solving the entire problem in the linearized approximation, since the addition of a constant to the potential does not affect the solution. However, its presence is necessary when attempting to fit the data, since there is no guarantee that the numerical method will generate a potential distribution with zero mean value.

Case Studied

The matching method was applied to the case described in Appendix A. A tape was available, which contained the ϕ values at iteration number 720; this tape was used to start the solution. A sequence of runs was then made, in which a total of 680 iterations were done. The ϕ-data at $K = 10$ (0.89 chords upstream of the leading edge) was fitted, at various stages, with a series

truncated at k = 10, m = 30. The fitting of the ϕ -data at K = 10 was updated prior to iteration numbers 1, 11, 21, 81, 141, 201, 261, 321 and 621. Thus, the updating was done very frequently through the first 320 iterations, was held constant for the next 300 iterations, and was updated once more for the final 60 iterations.

It was found during the first 320 iterations that the use of the radiation condition produced a much improved description of the flow upstream. Figure 8 shows the sonic-line locations at ρ = 2.133; note that these Mach number contours extend ahead of the blade row in a much more satisfactory fashion than do those of Figure 7, which pertain to a spanwise station slightly farther outboard. The station where the data were fitted is indicated on Figure 8. The portion of the sonic contour lying upstream of this station is shown as a broken line, because the Mach number calculation in this region contains inaccuracies introduced by the procedure of differencing the potential values. A preferable procedure would be to differentiate the series, but this additional effort was not felt to be warranted at present.

It should be pointed out that the mean-chord locations in Figure 8 lie along the resultant of U_∞ and ωr, which is the surface in which the boundary conditions are applied in the small-disturbance limit. The actual blade locations are at a substantial angle of incidence to these mean chord lines, for the case considered here.

Although the first 320 iterations showed a greatly improved upstream flow pattern, they did not remove the tendency for waves to propagate. Rather, it was found that the Mach number contours continued to move, each time the fit to the boundary values of ϕ at K = 10 was updated. This is illustrated in Figure 9, which shows the movement of the sonic line that constitutes the downstream half of the loop shown in Figure 8. This line propagates through the blade-to-blade channel, at a fairly constant speed, during the period when the fitted values are being updated.

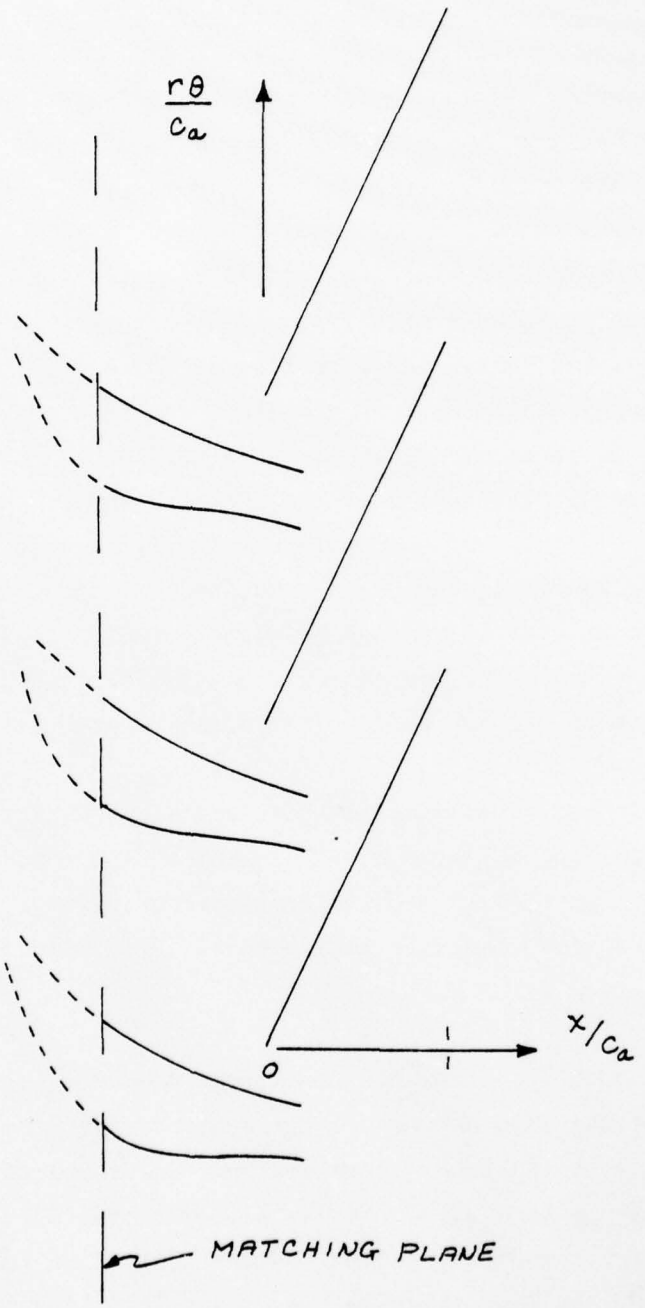

FIGURE 8 SONIC-LINE CONTOURS UPSTREAM OF THE BLADE ROW AFTER 140 ITERATIONS
$\rho = 2.1333$

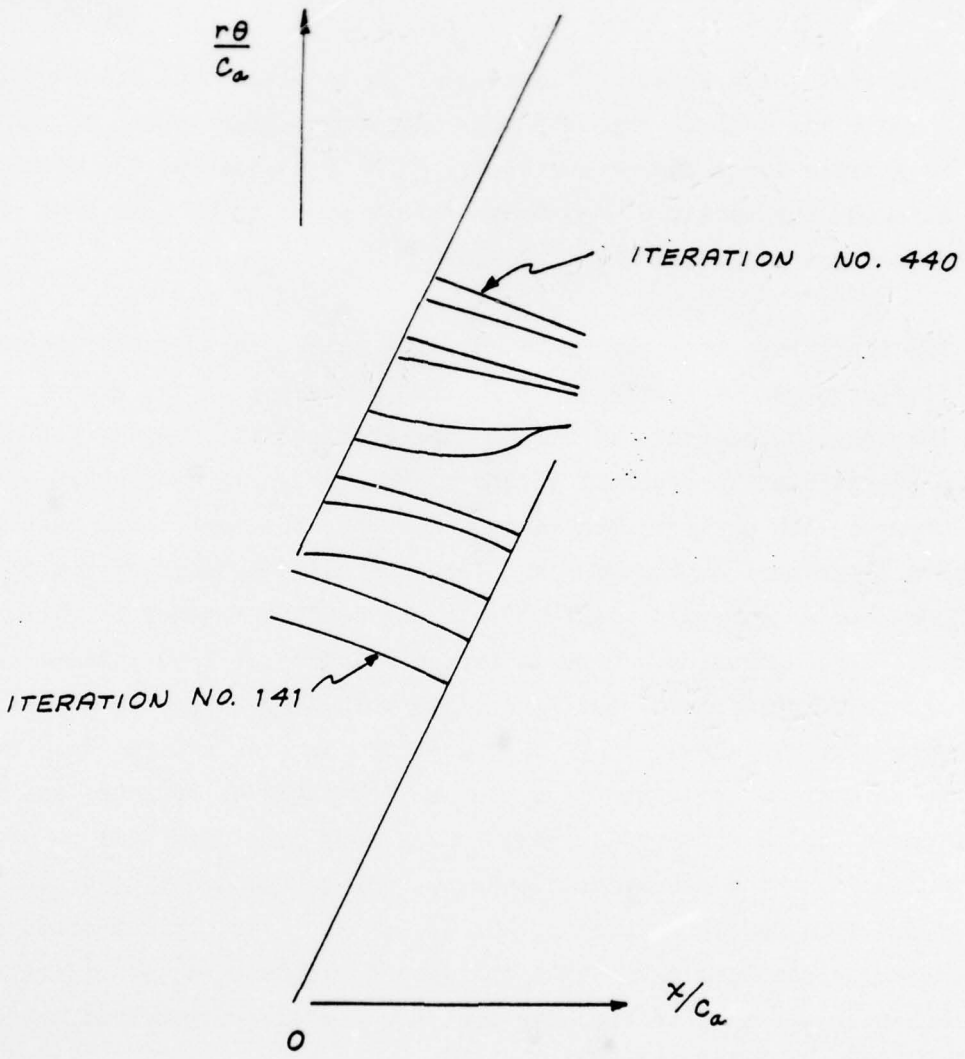

FIGURE 9 MOTION OF A SONIC-LINE CONTOUR. POSITIONS ARE SHOWN EVERY 30 ITERATIONS
$\rho = 2.1333$

The influence of the frequency of updating was examined next, by holding the fitted values constant for 300 iterations, and then releasing them one more time for the final 60 iterations. It was hoped that this procedure would allow the waves to pass out of the flow, so that the adjustment called for on the final update would be minimal.

The results are shown in Figure 10. It is clear that holding ϕ fixed at K = 8 and 9 has reduced substantially the amount of movement of the sonic line. A relatively large change occurs at K = 10 as soon as the fitting is updated, although the amount of movement overall seems to be less than observed during the previous stages of the iterations.

The iterations were terminated at this point, because the amount of computer time required was beginning to exceed the scope of the effort. On the basis of the results obtained, it does appear that the matching method has achieved a substantial improvement in the flowfield description ahead of the blades, compared with earlier treatments. However, the particular case chosen, and the particular choices made for the location and frequency of the updating, have not produced a converged solution. It may be that further iterations would lead to a converged solution, since it typically requires 1500 iterations or more for convergence of a subsonic case with comparable grid size. It may also be true that the initial values of ϕ , as well as the case chosen, are too severe a test; the initial solution contains many strong-gradient regions, and the large incidence angles involved suggest that strong gradients will be present in the final solution. Some consideration was given to the starting of an entirely new case, with more moderate loading, but it was felt that this procedure might require excessive computer time. The decision to attempt the stabilization of the previous case was made in the hope that a successful demonstration could be made with minimum computer cost.

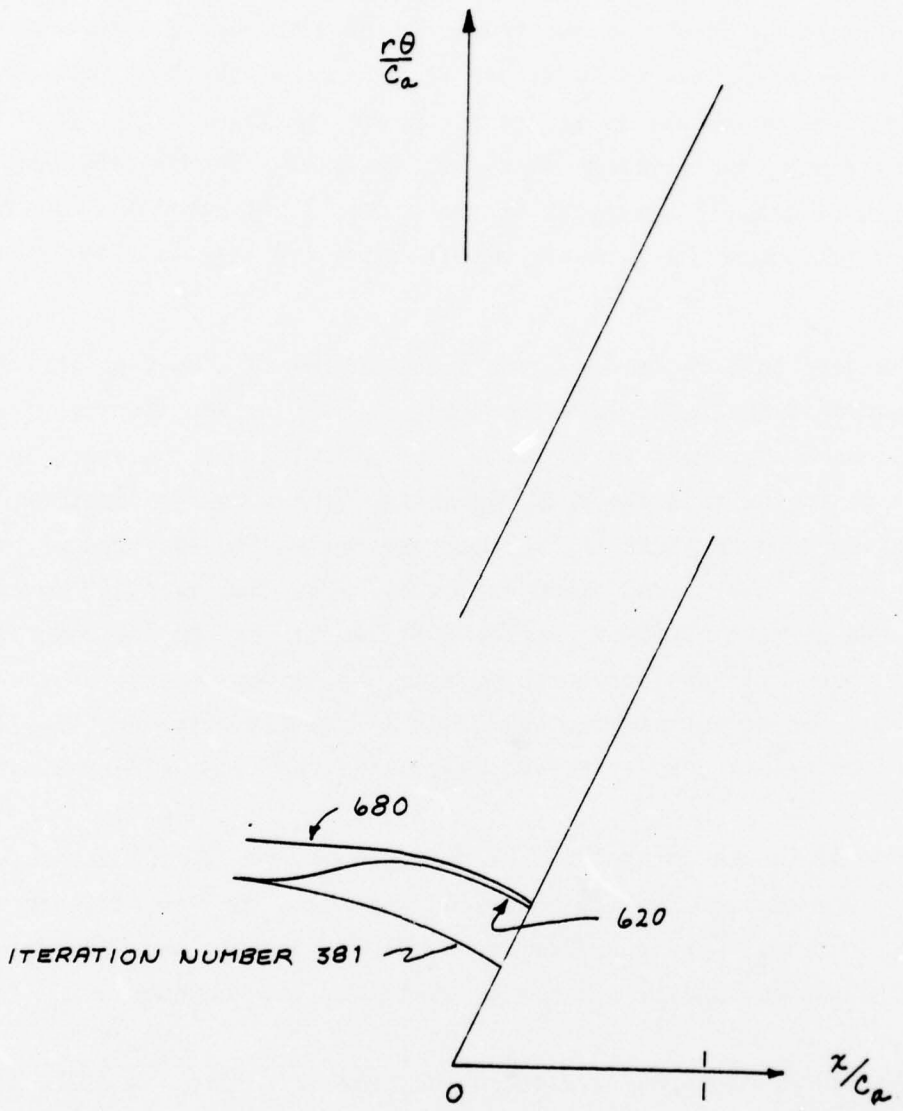

FIGURE 10 MOTION OF A SONIC LINE. FITTED POTENTIAL HELD CONSTANT FOR ITERATIONS 381 THROUGH 620, THEN UPDATED AT ITERATION 621
$\rho = 2.1333$

Section 5
CONCLUSIONS

Candidate approaches were examined for enforcing a radiation condition in numerical solutions of the transonic flow through a compressor rotor. The method of matching the analytic series solution with the numerical method was selected for incorporation into the computer program. This approach is in principle exact, and limited numerical trials have shown a physically realistic picture of the flow upstream of the rotor. What remains to be found is a convergent procedure for coupling the analytic and numerical portions of the calculation.

The test case chosen may have been too severe a test of the method, since it contained many steep-gradient regions. It is not clear whether the method would have converged if applied to a case with more moderate loading, and one which was started from the very beginning. The steep-gradient regions present in the solution used to start the sample case above were the product of 720 iterations done without a radiation condition. The fact that 680 further iterations with the correct boundary condition failed to restore the solution to convergence should perhaps not be surprising. In order to resolve the influence of the initial conditions and the magnitude of the disturbances, it will be necessary to do a less heavily loaded case, starting from uniform flow.

In addition to doing this new case, there are several other features of the procedure that warrant further study, namely, the use of fewer terms, application of other rules for carrying out the matching, and incorporation of a suitable radiation condition for the downstream grid boundary.

The number of terms carried in the present effort was 311. It is not clear whether use of the high-frequency portions of this set can be justified, since the numerical data is specified only at discrete points (for the case above, 10 radial stations and 13 in the blade-to-blade direction). A limited examination of the amplitude coefficients suggests that the series is dominated by about three to six terms. It would be interesting to see whether the results would be altered by dropping all but the dominant terms.

The rules used for effecting the matching were confined here to updating the potential at preselected intervals. There are many alternatives to this procedure that might have greater merit, such as the matching of velocity components rather than the potential, or the introduction of relaxation factors such that the fitted potential is made to respond only slowly to changes in the numerical data. In addition, there is insufficient experience to date on the effects of the frequency with which the fitting is done. It seems plausible that the fitted values should be left unchanged for as many iterations as are needed to carry information to the downstream edge of the grid (50 in the case above), but it is not known whether a longer period between updates would improve stability.

It should be repeated that the only case considered is that of subsonic exit flow. In practical applications, there may be cases where the flow exits at supersonic speeds. Extensions are needed, to provide a radiation condition applicable to these cases.

Finally, the ultimate goal is to learn about the phenomena that occur near the inlet of a three-dimensional transonic compressor. When this basic understanding is achieved, it may be possible to bypass the cumbersome parts of the matching method altogether, replacing them by simpler expressions that contain the essential physics in a manner more suited to flowfield computation.

REFERENCES

1. Adamson, T.C. and Platzer, M.F., eds. Transonic Flow Problems in Turbomachinery Hemisphere Publishing Corp., Washington (1977)

2. Benser, W.A., Bailey, E.E. and Gelder, T.F. "Holographic Studies of Shock Waves Within Transonic Fan Rotors" Paper presented at the ASME Nineteenth International Gas Turbine Conference, Zurich, Switzerland; available as NASA TM X-71430 (30 March - 4 April 1974)

3. Wisler, D.C. "Shock Wave and Flow Velocity Measurements in a High Speed Fan Rotor Using the Laser Velocimeter" ASME Paper 76-GT-49 (March 1976)

4. Gallus, H.E., Bohn, D. and Broichhausen, K.D. "Measurements of Quasi-Steady and Unsteady Flow Effects in a Supersonic Compressor Stage" ASME Paper 77-GT-13 (March 1977)

5. Dunker, R.J., Strinning, P.E. and Weyer, H.B. "Experimental Study of the Flow Field Within a Transonic Axial Compressor Rotor by Laser Velocimetry and Comparison with Through-Flow Calculations" ASME Paper 77-GT-28 (March 1977)

6. Alzner, E. and Erdos, J. "Unsteady Flow Through Compressor Stages" Advanced Technology Labs., Inc. Report TR-168 NASA CR-127765 (December 1971)

7. McDonald, P.W. "The Computation of Transonic Flow Through Two-Dimensional Gas Turbine Cascades" American Society of Mechanical Engineers, Paper 71-GT-89 (1971)

8. Gopalakrishnan, S. and Bozzola, R. "Computation of Shocked Flows in Compressor Cascades" American Society of Mechanical Engineers, Paper 72-GT-31 (1972)

9. Kurzrock, J.W. and Novick, A.S. "Transonic Flow Around Rotor Blade Elements" Transactions of the ASME Vol. 97 (December 1975) pp. 598-607

10. Erdos, J., Alzner, E. and McNally, W.D. "Numerical Solution of Periodic Transonic Flow Through a Fan Stage" AIAA Journal 15 No. 11 (November 1977) 1559-1568

11. Dodge, P.R. "A Transonic Relaxation Method for Cascade Flow Systems" von Karman Institute for Fluid Dynamics, Lecture Series on Transonic Flow in Turbomachinery (May 1973)

12. Shope, F.L. and Lakshminarayana, B. "Relaxation Solution of High Subsonic Cascade Flows and Extension of This Method to Transonic Cascades" AIAA Paper 75-23 (January 1975)

13. Luu, T.S. and Coulmy, G. "Relaxation Solution for the Transonic Flow Through a Cascade" Symposium Transsonicum II, edited by K. Oswatitsch and D. Rues, Springer-Verlag, Berlin, 1976, pp. 331-339

14. Dodge, P.R. "A Non-Orthogonal Transonic Relaxation Method for Cascade Flows" ASME Paper 76-GT-63 (March 1976)

15. Ives, D.C. and Liutermoza, J.F. "Analysis of Transonic Cascade Flow Using Conformal Mapping and Relaxation Techniques" AIAA Journal 15 No. 5 (May 1977) 647-652

16. Sator, F.G. "Computation of Transonic Flow with Detached Bow Shocks Through Two-Dimensional Turbomachinery Cascades" International Council of Aerospace Sciences, Paper 76-40 (October 1976)

17. Sator, F.G. "Inverse Computation of Profile Shapes for Given Transonic Flow Configurations, with and without Detached Bow Shocks in Two-Dimensional Turbomachinery Cascades" ASME Paper 77-GT-33 (March 1977)

18. Japiske, D. "Review-Progress in Numerical Turbomachinery Analysis" Journal of Fluids Engineering Trans ASME 98I (December 1976) 592-606

19. Novak, R.A. and Hearsey, R.M. "A Nearly Three-Dimensional Intrablade Computing System for Turbomachinery - Part I, General Description; Part II - System Details and Additional Examples" ASME Papers 76-FE-19 and 20 (March 1976)

20. Hirsch, C. and Warzee, G. "An Integrated Quasi-3D Finite Element Calculation Program for Turbomachinery Flows" ASME Paper 78-GT-56 (April 1978)

21. Oliver, D.A. "Four Issues in the Computation of Transonic Flows in Turbomachinery" pp. 163-165 of Ref. 1

22. Oliver, D.A. and Sparis, P. "Computational Aspects of the Prediction of Multidimensional Transonic Flows in Turbomachinery" pp. 567-585 of Aerodynamic Analyses Requiring Advanced Computers Part I, NASA SP-347 (1975)

23. Paris, D.S., Ganz, A.A. and Liutermoza, J.F. "Some Formulation Considerations in 3-D Transonic Flow Computation" pp. 79-94 of Ref. 1

24. Veuillot, J.P. "Calculation of the Quasi Three-Dimensional Flow in a Turbomachine Blade Row" Journal of Engineering for Power Trans. ASME 99 (A) (January 1977) pp. 53-62

25. Rae, W.J. "Calculations of Three-Dimensional Transonic Compressor Flow-fields by a Relaxation Method" Journal of Energy 1 (1977) 284-296

26. Rae, W.J. "Nonlinear Small-Disturbance Equations for Three-Dimensional Transonic Flow Through a Compressor Blade Row" AFOSR TR-76-1082 AD-A031234 (August 1976)

27. Rae, W.J. "Relaxation Solutions for Three-Dimensional Transonic Flow Through a Compressor Blade Row, in the Nonlinear Small-Disturbance Approximation" AFOSR TR-76-1081, AD-A032553 (August 1976)

28. Rae, W.J. "Computer Program for Relaxation Solutions of the Nonlinear Small-Disturbance Equations for Transonic Flow in an Axial Compressor Blade Row" Calspan Report No. AB-5487-A-3 (April 1978)

29. Rae, W.J. "Finite-Difference Calculations of Three-Dimensional Transonic Flow Through a Compressor Blade Row, Using the Small-Disturbance Nonlinear Potential Equation" pp. 228-252 of Ref. 1

30. Murman, E.M. and Cole, J.D. "Calculation of Plane Steady Transonic Flows" AIAA Journal 9 pp. 114-121 (1971)

31. McCune, J.E. "The Three-Dimensional Flow Field of an Axial Compressor Blade Row-Subsonic, Transonic, and Supersonic" Ph.D. Thesis Cornell University (February 1958)

32. McCune, J.E. "A Three-Dimensional Theory of Axial Compressor Blade Rows - Application in Subsonic and Supersonic Flows" Journal of the Aerospace Sciences Vol. 25 No. 9 (September 1958) pp. 544-560

33. McCune, J.E. "The Transonic Flow Field of an Axial Compressor Blade Row" Journal of the Aerospace Sciences Vol. 25 No. 10 (October 1958) pp. 616-626

34. Okurounmu, O. and McCune, J.E. "Three-Dimensional Vortex Theory of Axial Compressor Blade Rows at Subsonic and Transonic Speeds" AIAA Journal Vol. 8 No. 7 (July 1970) pp. 1275-1283

35. Okurounmu, O. and McCune, J.E. "Lifting Surface Theory of Axial Compressor Blade Rows: Part I - Subsonic Compressor; Part II - Transonic Compressor" AIAA Journal 12 (October 1974) pp. 1363-1380

36. Lordi, J.A. "Report on a Study of Noise Generation by a Rotating Blade Row in an Infinite Annulus" U.S. Air Force Office of Scientific Research Scientific Report AFOSR TR-71-1485; also available as Calspan Report No. AI-2836-A-1 (May 1971)

37. Lordi, J.A. "Noise Generation by a Rotating Blade Row in an Infinite Annulus" AIAA Paper No. 71-617 AIAA 4th Fluid and Plasma Dynamics Conference, Palo Alto, California (21-23 June 1971)

38. Thompkins, W.T. and Epstein, A.H. "A Comparison of the Computed and Experimental Three-Dimensional Flow in a Transonic Compressor Rotor" AIAA Paper 76-368 (July 1976)

39. Magnus, R.J. "Computational Research on Inviscid, Unsteady, Transonic Flow over Airfoils" Convair Division of General Dynamics Report CASD/LVP 77-010 (January 1977)

40. Schwenk, F.C., Lewis, G.W. and Hartmann, M.J. "A Preliminary Analysis of the Magnitude of Shock Losses in Transonic Compressors" NACA RM E57A30 (March 1957)

41. Miller, G.R. and Bailey, E.E. "Static-Pressure Contours in the Blade Passage at the Tip of Several High Mach Number Rotors" NASA TM X-2170 (February 1971)

42. Levine, P. "Two-Dimensional Inflow Conditions for a Supersonic Compressor with Curved Blades" Journal of Applied Mechanics 24 (1957) pp. 165-169

43. Fink, M.R. "Shock Wave Behavior in Transonic Compressor Noise Generation" Trans ASME 93 (D) Journal of Engineering for Power No. 4 (October 1971) 397-403

44. Lichtfuss, H.J. and Starken, H. "Supersonic Cascade Flow" pp. 37-149 of Progress in Aerospace Sciences Vol. 15 ed. by D. Kuchemann Pergamon Press, New York (1974)

45. Jameson, A. "Iterative Solution of Transonic Flows over Airfoils and Wings, Including Flows at Mach 1" Communications on Pure and Applied Mathematics 27 pp. 283-309 (1974)

46. Yu, N.J., Seebass, A.R. and Ballhaus, W.F. "An Implicit Shock-Fitting Scheme for Unsteady Transonic Flow Computations" AIAA Paper 77-633 (June 1977)

47. Fung, K.Y., Yu, N.J. and Seebass, A.R. "Small Unsteady Perturbations in Transonic Flows" AIAA Paper 77-675 (June 1977)

48. Seebass, A.R., Yu, N.J. and Fung, K.Y. "Unsteady Transonic Flow Computations" Paper presented at the AGARD Fluid Dynamics Panel Symposium on Unsteady Aerodynamics, Ottawa, Canada (September 1977)

APPENDIX A

BLADE GEOMETRY AND OPERATING CONDITIONS
FOR THE CASE DESCRIBED IN SECTIONS 3 AND 4

The blade geometry and operating conditions were patterned after the MIT rotor, described in Reference 38. That blade row has 23 blades, with a hub-to-tip ratio of 0.5, an axial Mach number of 0.5, and a circumferential Mach number at the tip of 1.2 (making the resultant Mach number at the tip equal to 1.3). The blade geometry and orientation are given in the table below, where the notation defining the various angles with respect to the mean camber line is (Reference A-1, p. 228).

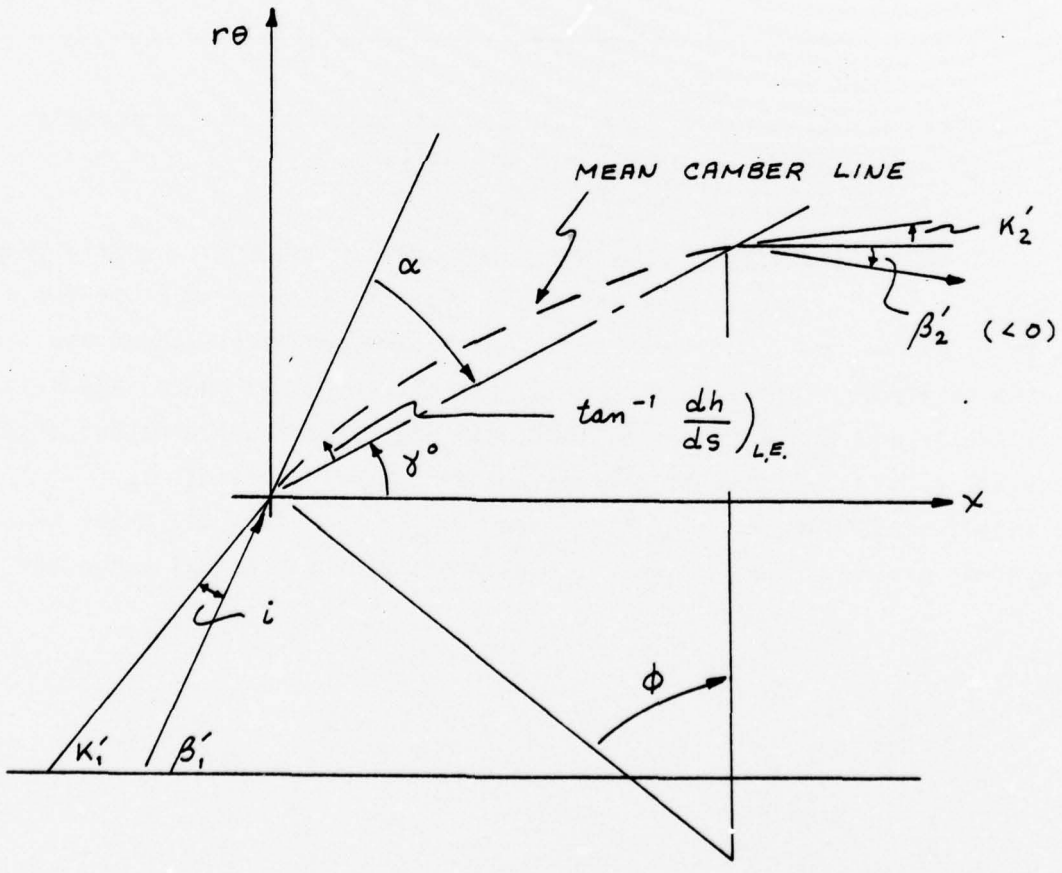

A-1 Johnsen, I.A. and Bullock, R.O., eds. Aerodynamic Design of Axial-Flow Compressors NASA SP-36 (1965)

Table 1. ROTOR SPECIFICATIONS

r/r_T	t_{MAX}/c	$\sigma = \frac{c/2\pi r}{23}$	β_1'	K_1'	$\gamma°$	i	K_2'	ϕ
.5	.10	2.0	50.19°	38.7°	28.9°	11.5°	16.7°	22.0°
.6	.086	1.67	55.22	44.8	38.1	10.4	30.1	14.7
.7	.072	1.43	59.24	49.3	45.0	9.1	40.3	9.0
.8	.058	1.25	62.49	55.0	51.1	7.5	47.5	7.5
.9	.044	1.11	65.16	61.2	56.3	4.0	54.1	7.1
1.0	.030	1.00	67.38	66.1	61.7	1.3	58.0	8.1

Here r_T denotes the tip radius, t_{MAX} the maximum thickness at the prescribed radius, c the local chord length, and σ the solidity.

These blades had a constant value of c, and their profile shape consisted of multiple circular arc sections. For the present work, it was necessary to choose some equivalent shape, since the computer program used was restricted to blades with a constant axial projection of the chord, and also to double-circular-arc distributions of thickness and camber, which differ slightly from the MIT rotor. In order to choose representative values of c_a/L_T, and of the radial variations of t_{MAX}/c_a and h_{MAX}/c_a, the following table was prepared, giving values derived from parameters of the actual blade row:

r/r_T	ρ	c/c_a	t_{MAX}/c_a	c_a/L_T	h_{MAX}/c_a	α
.5	1.20	1.56	.156	.640	.0759	21.3°
.6	1.44	1.75	.151	.572	.0565	17.1
.7	1.68	1.96	.141	.512	.0385	14.2
.8	1.92	2.16	.126	.462	.0355	11.4
.9	2.16	2.38	.105	.420	.0369	8.9
1.0	2.40	2.60	.078	.385	.0460	5.7

These values were found from the following formulas:

$$\rho = \frac{\omega r}{U_\infty} = \frac{M_\theta}{M_x} = \tan\beta_1' \; ; \; \frac{c}{c_a} = \sqrt{1+\rho^2} \; ; \; \frac{t_{MAX}}{c_a} = \frac{t_{MAX}}{c} = \frac{c}{c_a}$$

$$\frac{c_a}{L_T} = \sigma \cdot \frac{c_a}{c} \cdot \frac{r}{r_T} \; ; \; \alpha = \beta_1' - \gamma°$$

$$\frac{h_{MAX}}{c_a} = \frac{\sqrt{1+\rho^2}}{4} \tan\left(\frac{\phi}{2}\right) \; ; \; \phi = K_1' - K_2'$$

The basis for the last of these formulas is that, for a blade profile that is symmetric fore and aft about the midchord, the camberline slopes are:

$$\phi = 2\tan^{-1}\left.\frac{dh}{ds}\right)_{L.E.} = 2\tan^{-1}\left\{\frac{4}{\sqrt{1+\rho^2}} \cdot \frac{h_{MAX}}{c_a}\right\}$$

On the basis of these values, the calculations were made with the constant value $c_a/L_T = 0.5$, and the angle of attack and maximum thickness and camber were taken as

$$\alpha = 18.9^\circ + \frac{6.0^\circ}{R} - 19.2^\circ R \quad ; \quad R \equiv \frac{r}{r_T} = \frac{\rho}{\rho_T}$$

$$\frac{h_{MAX}}{c_a} = -0.3620 + \frac{0.1560}{R} + 0.2520\,R$$

$$\frac{t_{MAX}}{c_a} = 0.5227 - \frac{0.0960}{R} - 0.3480\,R$$

These fitted values compare with the actual ones as follows:

	α		h_{MAX}/c_a		t_{MAX}/c_a	
R	Actual	Fitted	Actual	Fitted	Actual	Fitted
.5	21.3°	21.3°	.0759	.0760	.156	.157
.6	17.1	17.4	.0565	.0492	.151	.154
.7	14.2	14.0	.0385	.0373	.141	.142
.8	11.4	11.0	.0355	.0346	.126	.124
.9	8.9	8.3	.0369	.0381	.105	.103
1.0	5.7	5.7	.0460	.0460	.078	.079

These values of thickness and camber are not markedly different from those used in previous small-distrubance calculations.[25] However, the values assigned to the angle of attack are quite large, especially near the hub, and obviously extend beyond the range of validity of the small-disturbance equations.

APPENDIX B

LIMITATIONS OF THE PARABOLIC APPROXIMATION IN TRANSONIC COMPRESSOR FLOWS

Section 3 contains a brief description of a method for including an approximate representation of nonlinear transonic effects in the linearized analysis of the three-dimensional flow through an axial compressor blade row, in which the transonic small disturbance equation is linearized by introducing an approximation analogous to the parabolic method used for external transonic flows. This approach removes the transonic resonance which appears in the fully linearized solution for the rotor flow field. The source solution of the modified linear equation for the velocity potential was derived, and the thickness contribution to the rotor flow field in this approximation was obtained by superposition of the source solutions. Our previous work[B-1] on the calculation of the acoustic spectrum of a transonic rotor demonstrated that the blade thickness effects dominate the sound field, and so, given the restricted applicability of the modified linear theory, it was decided to proceed with numerical evaluations of the thickness contributions, rather than carrying the parabolic approximation farther, to include the loading contributions.

In this appendix, the limitations of the parabolic approximation for compressor flows are discussed first. Then the results of the calculations with the modified linear theory are described.

The equations governing the three-dimensional, small disturbance, transonic flow through a rotor in a cylindrical annulus have been derived in Refs. 26 and 35. The flow is assumed steady in coordinates fixed to the blade row so that the undisturbed relative inflow is composed of a constant axial component,

---

[B-1] Lordi, J.A, Homicz, G.F. and Ludwig, G.R. "Investigation of Rotating Stall Phenomena in Axial-Flow Compressors, Vol. II - Investigation of Rotor-Stator Interaction Noise and Lifting Surface Theory for a Rotor" Calspan Report No. XE-5315-A-12 AFAPL TR-76-49 Vol. II (June 1976)

u_∞, and a tangential component, ωr. The coordinate system and perturbation velocity components are defined in Figure 1. The velocity potential satisfies the equation

$$\beta^2 \bar{\Phi}_{zz} + \bar{\Phi}_{\rho\rho} + \frac{1}{\rho}\bar{\Phi}_\rho + \frac{1}{\rho^2}(1 - M_\infty^2 \rho^2)\bar{\Phi}_{\theta\theta} - 2M_\infty^2 \bar{\Phi}_{\theta z}$$

$$= \frac{(\gamma+1)M_\infty^2}{1+\rho^2}(\bar{\Phi}_z + \bar{\Phi}_\theta)(\bar{\Phi}_{zz} + 2\bar{\Phi}_{z\theta} + \bar{\Phi}_{\theta\theta}) \qquad \text{(B-1)}$$

where

$$z = \frac{\omega x}{u_\infty} \qquad \rho = \frac{\omega r}{u_\infty}$$

$$\bar{\Phi}_z = \frac{u}{u_\infty} \qquad \bar{\Phi}_\rho = \frac{v}{u_\infty} \qquad \frac{1}{\rho}\bar{\Phi}_\theta = \frac{w}{u_\infty} \qquad \text{(B-2)}$$

$$\beta^2 = 1 - M_\infty^2 \qquad M_\infty = \frac{u_\infty}{a_\infty}$$

The terms on the right hand side of Equation (1) are those nonlinear terms which become important when the relative Mach number, $M_R = \sqrt{u_\infty^2 + (\omega r)^2}/a_\infty$, is near unity.

Introducing the parabolic approximation to the nonlinear terms on the right hand side of Equation (B-1), the equation for the velocity potential is written

$$\beta^2 \bar{\Phi}_{zz} + \bar{\Phi}_{\rho\rho} + \frac{1}{\rho}\bar{\Phi}_\rho + \frac{1}{\rho^2}(1 - M_\infty^2 \rho^2)\bar{\Phi}_{\theta\theta} - 2M_\infty^2 \bar{\Phi}_{\theta z} = \Lambda(\bar{\Phi}_z + \bar{\Phi}_\theta) \qquad \text{(B-3)}$$

where

$$\Lambda = \frac{(\gamma+1)M_\infty^2}{1+\rho^2}(\bar{\Phi}_{zz} + 2\bar{\Phi}_{z\theta} + \bar{\Phi}_{\theta\theta}) \qquad \text{(B-4)}$$

is assumed constant. With Λ constant, the equation for the potential is still separable and has the following eigenfunction solutions

$$\bar{\Phi}_{n\ell} = A_{n\ell} R_{n\ell}(K_{n\ell}\sigma) e^{in\theta} \exp\left\{\left[\frac{in M_\infty^2}{\beta^2} + \frac{1}{\beta^2}\left(\frac{\Lambda}{2}\right) \pm \bar{\lambda}_{n\ell}\right] z\right\} \qquad \text{(B-5)}$$

where

$$\bar{\lambda}_{nk} \equiv \sqrt{\lambda_{nk}^2 + \left(\frac{\Lambda}{2\beta^2}\right)^2 + \frac{2in}{\beta^2}\left(\frac{\Lambda}{2\beta^2}\right)} \tag{B-6}$$

and λ_{nk} is given by

$$\lambda_{nk} = \frac{n}{\rho_T \beta^2}\sqrt{\beta^2\left(\frac{K_{nk}}{n}\right)^2 - M_T^2} \tag{B-7}$$

The quantity R_{nk} is the radial eigenfunction which is a normalized combination of the Bessel and Neumann functions of order n. Also, K_{nk} is the k^{th} radial eigenvalue for any n and M_T is defined as $\omega r_T / a_\infty$. The subscript T refers to values at the tip radius, and $\sigma = \rho/\rho_T$ is the normalized radial coordinate, having a value of h at the hub wall and unity at the outer wall.

In order to choose the proper branches of the solution, the argument of the exponential is separated into its real and imaginary parts.

$$\bar{\lambda}_{nk} = |\bar{\lambda}_{nk}|\left[\cos\left(\frac{\Theta_{nk}}{2} + l\pi\right) + i\sin\left(\frac{\Theta_{nk}}{2} + l\pi\right)\right] \qquad l = 0, 1 \tag{B-8}$$

where

$$|\bar{\lambda}_{nk}| = \left\{\left[\lambda_{nk}^2 + \left(\frac{\Lambda}{2\beta^2}\right)^2\right]^2 + \left[\frac{2n}{\beta^2}\left(\frac{\Lambda}{2\beta^2}\right)\right]^2\right\}^{1/4} \tag{B-9}$$

$$\Theta_{nk} = \tan^{-1}\left\{\frac{2n}{\beta^2}\left(\frac{\Lambda}{2\beta^2}\right) \Big/ \left[\lambda_{nk}^2 + \left(\frac{\Lambda}{2\beta^2}\right)^2\right]\right\} \tag{B-10}$$

Initially, the branches of $\bar{\lambda}_{nk}$ were chosen so that the eigenfunction solutions decay for $z \to \pm\infty$. This procedure was followed for all values of M_T, both above and below the value $M_T = \beta K_{nk}/n$, which corresponds to the resonance condition in the fully linearized limit ($\Lambda \longrightarrow 0$).
In the linearized case, the modes below resonance are quickly damped with distance from the rotor. Above resonance the modal solutions represent undamped

waves, and the proper branch of the solution is chosen on the basis of outward propagation away from the rotor. The parabolic approximation for the nonlinear transonic term introduces the equivalent of a damping term into the governing equation for the potential. Accordingly, the eigenfunction solutions given in Equation (B-5) are damped both above and below the resonance condition for the linearized case. It was discovered, however, that choosing the branches of λ_{nk} so that the solutions decay does not give physically meaningful results.

The relationship given in Equation (B-4) can be used to express Λ as

$$\Lambda = -\frac{(\gamma+1)\,M_\infty^2}{1+\rho^2}\left.\frac{\partial}{\partial \bar{z}}\right)_{\zeta,\rho}\left(\frac{p}{\rho_\infty U_\infty^2}\right) \tag{B-11}$$

where p is the perturbation pressure and ζ the helical coordinate, $\zeta = \theta - \bar{z}$ Tha damping rates for the modal solutions were evaluated with a value of Λ based on Equation (B-11) and the average pressure rise through the rotor. The resulting value of Λ is negative, and so, from Equation (B-10), $\theta_{nk}/2$ can be seen to lie in the fourth quadrant. The factor in the eigenfunction solution which describes the decay with axial distance from the rotor is

$$\alpha_{nk} = \exp\left[\left(\frac{\Lambda}{2\beta^2} \pm \left|\bar{\lambda}_{nk}\right| \cos\frac{\theta_{nk}}{2}\right)\bar{z}\right] \tag{B-12}$$

where the plus sign corresponds to the $l=0$ branch of $\bar{\lambda}_{nk}$ and the minus sign corresponds to the $l=1$ branch. Decaying solutions are obtained by applying the $l=0$ branch for $\bar{z}<0$ and the $l=1$ branch for $\bar{z}>0$.

The numerical evaluations of α_{nk} demonstrated that the above form approaches the linearized result away from resonance. The linearized result can also be recovered analytically.

For $\Lambda \to 0$,

$$\left|\bar{\lambda}_{nk}\right| \to \sqrt{\left|\lambda_{nk}^2\right|}$$

For M_T well below the resonance, $\theta_{n\ell}/2 \to 0$ and $\lambda^2_{n\ell} > 0$, so

$$\lim_{\Lambda \to 0} \alpha_{n\ell} = e^{\pm\sqrt{|\lambda^2_{n\ell}|}\, z} = e^{\pm \lambda_{n\ell} z}$$

which is the linearized result. For M_T well above the resonance value, $\theta_{n\ell}/2 \longrightarrow -\pi/2$, and so $\alpha_{n\ell} \to 1$ which corresponds to the linearized limit of no damping above resonance. The difficulty arises when trying to recover the linearized result for the propagation factors in the eigenfunction solutions.

Above resonance, $M_T > \beta K_{n\ell}/n$ and $\lambda^2_{n\ell} < 0$. The linearized eigenfunction solutions, transformed from the blade-fixed coordinates to duct-fixed coordinates by setting $\theta = \theta_d + \omega t$, take the form

$$\Phi_{n\ell} = A_{n\ell} R_{n\ell}(K_{n\ell}\sigma) e^{in\theta'} \exp\left[\left(\frac{in M_\infty^2}{\beta^2} \pm i\sqrt{|\lambda^2_{n\ell}|}\right) z + in\omega t\right] \tag{B-13}$$

The argument of the second exponential factor describes the wave propagation in the axial direction. Far above the resonance condition, i.e. for $M_T^2 >> (\beta K_{n\ell}/n)^2$, the choice of the plus sign can be shown to lead to a phase velocity in the z direction of $u_\infty - a_\infty$; the minus sign yields a phase velocity of $u_\infty + a_\infty$. Therefore, the plus sign applies for $z < 0$ and the minus sign applies for $z > 0$ in order to have outward propagating waves.

In the parabolic approximation, the exponential factor which represents propagation in the axial direction is

$$\exp\left[\left(\frac{in M_\infty^2}{\beta^2} \pm i\left|\overline{\lambda_{n\ell}}\right| \sin\frac{\theta_{n\ell}}{2}\right) z + in\omega t\right]$$

where, again, the plus sign corresponds to the $\ell = 0$ branch of $\bar{\lambda}_{n\ell}$. Now, when $\Lambda \longrightarrow 0$ from negative values, $|\overline{\lambda_{n\ell}}| \longrightarrow \sqrt{|\lambda^2_{n\ell}|}$ and $\theta_{n\ell}/2 \longrightarrow -\pi/2$. If the branches are chosen to be consistent with the modes being damped, then the signs in the propagation factor are opposite from those in the linearized limit. In other words, if the branches of $\overline{\lambda_{n\ell}}$ are selected so that the eigenfunction solutions decay, then the propagation factors correspond to inward moving waves. Conversely, if the branches are chosen to give outward propagating waves, the solutions grow exponentially with distance from the rotor.

The reason for this behavior of the eigenfunction solutions has been traced to the fact that negative values of Λ imply a "negative damping" in the equation for the potential. It has been verified that with positive values of Λ, the branches of $\bar{\lambda}_{n\ell}$ which lead to decaying modes also correspond to outward propagation. That this implies positive damping can be seen from discussions of the procedure of inserting a damping term in the wave equation in order to enforce a radiation condition, *see for example the discussion by Noble.*[B-2]

Despite this restriction on the applicability of the parabolic method to the flow through a transonic rotor, calculations within this approximation are still expected to be worthwhile. Such calculations provide information about how far ahead of the rotor the flow is composed only of propagating duct modes, and also, how many terms in the eigenfunction solutions need to be included to describe accurately the inlet flow. Since the information to be gained is more qualitative than quantitative, however, the evaluations with the modified linear theory are confined to the blade thickness effects. The results of such calculations are described next.

Flow Field of a Nonlifting Rotor in the Parabolic Approximation

Once the transonic small disturbance equation is linearized using the parabolic approximation, thickness and loading effects can be separated. A

[B-2] Noble, B. Methods Based on the Wiener-Hopf Technique Pergamon Press (1958) pp. 27-31

solution for the thickness contribution in this approximation was obtained by first finding the solution to Equation (B-1) for a point source, and then superimposing the solutions to obtain the result for B equally spaced blades as

$$\Phi = \sum_{j=1}^{B} \iint_{S_B} \Delta v_n(r_o, x_o)\, \Phi_s(r, \zeta, x; r_o, \zeta_o = \frac{2\pi j}{B}, x_o)\, d S_B \tag{B-14}$$

The thickness-only part of the solution requires that the local blade loading be zero and that the normal velocity component be given by

$$\Delta v_n = \sqrt{1+\rho^2}\, \frac{\partial t}{\partial s} \tag{B-15}$$

where $t = t(s, r)$ is the blade thickness, and S is the distance along the helical undisturbed streamlines. In the small disturbance approximation, the blade boundary conditions are satisfied on the undisturbed stream surfaces, $\zeta = 2\pi j / B$, $j = 1, 2, \ldots, B$.

In the calculations of the rotor flow field to be carried out, as in previous work on the linearized theory and in numerical solutions with the transonic small disturbance code, the thickness distribution is factored into a radial and axial variation so that

$$\frac{\partial t}{\partial s_o} = f(\sigma_o)\, g(z_o) \tag{B-16}$$

Introducing this form for the thickness distribution, specializing the expression to points upstream and downstream of the blade row ($z < 0$ and $z > \omega C_a / U_\infty$, respectively), the result for the potential was given as

$$\Phi^{u,d} = -\frac{B}{2\pi\beta^2\rho_T}\left[\frac{2}{1-k^2} F G^{u,d} + \frac{1}{2}\sum_{k=1}^{\infty} \frac{R_{ok}(\sigma)}{\lambda_{ok}} F_{ok} G_{ok}^{u,d}(z)\right.$$

$$\left. + R.P. \sum_{m=1}^{\infty}\sum_{k=1}^{\infty} \frac{R_{mBk}(\sigma)}{\lambda_{mBk}} e^{imB\zeta} F_{mk} G_{m,k}^{u,d}(z)\right] \tag{B-17}$$

where $$F = \int_h^1 f(\sigma_0)(1+\rho_T^2\sigma_0^2)\, d\sigma_0$$

$$F_{mk} = \int_h^1 f(\sigma_0)(1+\rho_T^2\sigma_0^2) R_{mB,k}(\sigma_0)\, d\sigma_0$$

$$G^u = 0 \qquad \text{(B-18)}$$

$$G^d = -\int_0^{\delta_a} g(z_0)(z-z_0)\, dz_0$$

$$G^{ud}_{0,k} = \int_0^{\delta_a} g(z_0)\, e^{\pm \lambda_{0k}(z-z_0)}\, dz_0$$

$$G^{u,d}_{m,k} = \int_0^{\delta_a} g(z_0)\, exp\left[\left(\frac{imB}{\beta^2} + \frac{\Lambda}{2\beta^2} \pm \bar{\lambda}_{mBk}\right)(z-z_0)\right] dz_0$$

The upper limit of the chordwise integrals, δ_a , is $\omega c_a / U_\infty$ where c_a is the axial projection of the blade chord that is assumed independent of radius. The superscript u and the + sign apply to points upstream of the rotor, the superscript d and the - sign apply downstream of the rotor, and $\bar{\lambda}_{mBk}$ refers to the $l = 0$ branch from here on. Here the $m = 0$ terms have been replaced by their linearized limit. The introduction of the approximate representation of the transonic nonlinear terms only affects the damping rates for these modes and, for the values of Λ based on the average pressure rise, there was virtually no difference between the linearized and parabolic method evaluation of the $m=0$ attentuation factors.

The velocity components are given by

$$\begin{bmatrix} \bar{u} \\ \bar{v} \\ \bar{w} \end{bmatrix} = -\frac{B}{2\pi\beta^2\rho_T} \left\{ \frac{1}{2} \sum_{k=1}^{\infty} R_{0k}(\sigma) \begin{bmatrix} U_{0,k}^{\pm} \\ V_{0k} \\ W_{0k} \end{bmatrix} F_{0k}\, G^{u,d}_{0k}(z)$$

$$+ \text{R.P.} \sum_{m=1}^{\infty} \sum_{k=1}^{\infty} R_{m\beta k}(\sigma)\, e^{im\beta\zeta} \begin{bmatrix} U^{\pm}_{m\beta k} \\ V_{m\beta k} \\ W_{m\beta k} \end{bmatrix} F_{mk}\; G^{u,d}_{mk}(z) \Bigg\} \tag{B-19}$$

where $\bar{u}, \bar{v}, \bar{w}$ are the velocity components normalized by U_∞ ,

$$U^{\pm}_{0,k} = \pm 1 \;, \quad V_{0,k} = \beta \frac{R'_{0k}(\sigma)}{R_{0k}(\sigma)} \;, \quad W_{0k} = 0 \tag{B-20a}$$

and, writing n for $m\beta$,

$$U^{\pm}_{nk} = \left(\frac{in M_\infty^2}{\beta^2} + \frac{\Lambda_-}{2\beta^2} \pm \bar{\lambda}_{nk} \right) \frac{1}{\bar{\lambda}_{nk}}$$

$$V_{nk} = \frac{K_{nk}}{\rho_T \bar{\lambda}_{nk}} \cdot \frac{R'_{nk}(\sigma)}{R_{nk}(\sigma)} \tag{B-20b}$$

$$W_{nk} = \frac{in}{\rho \bar{\lambda}_{nk}}$$

A computer code has been developed to evaluate the above flow-field expressions for rotor blades having similar parabolic-arc chordwise thickness distributions at each radial station. In this case $\partial t / \partial s$ is given by

$$\frac{\partial t}{\partial s} = 4\, \tau(\sigma) \left(1 - \frac{2z}{\delta_a} \right) \tag{B-21}$$

where $\tau(\sigma)$ is the ratio of the maximum thickness to the chordlength at each radius σ , and is assumed to be described by a polynomial in σ. The factors f and g defined by Equation (B-16), which describe the radial and axial dependence of $\partial t / \partial s$, can be identified as

$$f(\sigma_o) = \tau(\sigma_o) \qquad g(z_o) = f\left(1 - \frac{2z_o}{\delta_a} \right) \tag{B-22}$$

The choices made for the forms of f and g permit the radial and chordwise integrals F_{mk} and $G^{u,d}_{mk}$ to be evaluated analytically. The latter are easily evaluated in closed form. The former can be expressed as Lommel functions, which are calculable from either a terminating series or an asymptotic series.

The calculations which are presented below were carried out for a thickness-ratio variation given by

$$\tau(\sigma_o) = \tau_o \frac{1 + h^2 \rho_T^2}{1 + \sigma_o^2 \rho_T^2} \qquad \text{(B-23)}$$

where τ_o is the thickness ratio at the hub. This radial variation of the maximum thickness-to-chord ratio is such that the maximum thickness, t_{max}, decreases gradually from hub to tip. For example, with a hub-to-tip ratio of 0.5 and a value of ρ_T in the range 2-3, which is typical of transonic rotors with subsonic inflows, the maximum thickness at the blade tip is about .6 of the value at the hub.

Calculations of the velocity potential and the perturbation velocity components have been made for a rotor of 30 blades having the thickness distribution described above. The hub-to-tip radius ratio, h, was chosen to be .5, and the solidity parameter, c_a / ℓ_T, was also chosen to be 0.5. The axial flow Mach number, M_∞, was chosen to be 0.4 and the Mach number based on rotor tangential speed at the blade tips, M_T, was set at 1.2; the corresponding Mach number of the relative inflow, M_R, varies from 0.72 at the hub to 1.26 at the blade tips.

In the initial set of calculations, 10 terms were included in the sum over m and 20 terms were kept in the sum over k, in Equations (B-17 and (B-19). Results for the variation of the velocity component along the undisturbed streamline direction, v_s, are shown in Figure B-1. There the quantity $v_s / U_R \tau_o$, which is the negative of $p / \rho_\infty U_R^2 \tau_o$, is shown as a function of the helical coordinate ζ, for a dimensionless radius, σ, of 0.9 and for several chordwise stations upstream of the rotor. The values of ζ of 0 and $2\pi/B$ represent the undisturbed streamsurfaces on which the blades labeled $j = 0$ and $j = 1$ lie.

For the selected operating conditions, the first two radial modes ($k = 1$ and 2) are above the linearized resonance condition and hence would propagate in the duct; for $m = 10$, the first 14 radial modes will

FIGURE B-1 STREAMWISE VELOCITY COMPONENT UPSTREAM OF ROTOR

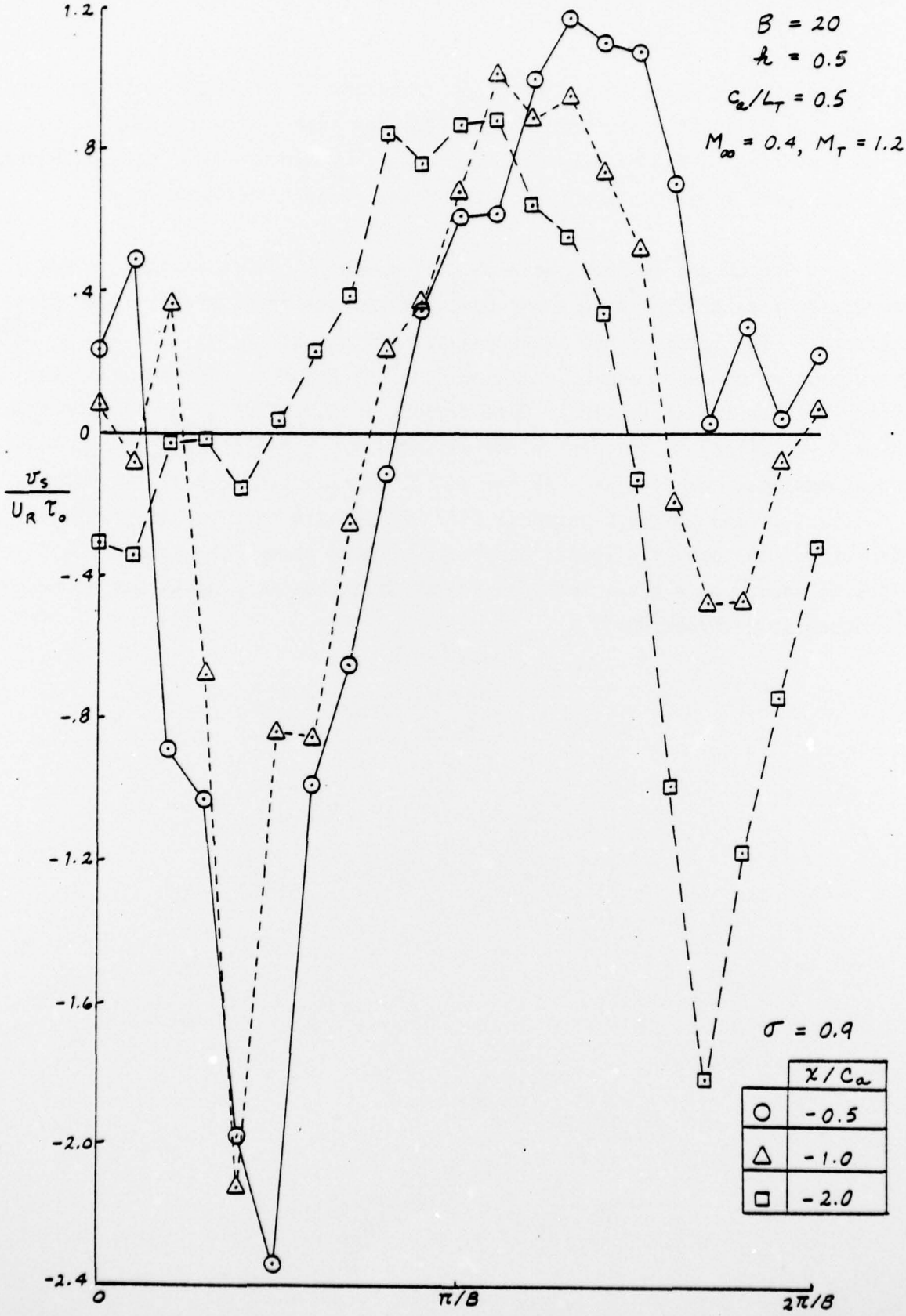

propagate. These modes of the solution represent the dominant contributions to the flow field at upstream distances greater than one blade chord. The results plotted in Figure B-1 show that a complicated pressure pattern develops, which contains several harmonics of the blade passage frequency.

One of the features we wish to look for in these results is the emergence of a pattern which shows how disturbances move upstream away from the rotor. The locus of the large negative values of v_s at $\zeta = \frac{2\pi}{5B} + \frac{2\pi j}{B}$ in successive blade passages, lie almost on the local two-dimensional Mach lines for this radial station. This feature is illustrated in Figure B-2 where these ζ locations in adjacent blade passages are shown along with the local two-dimensional Mach angles. At the radial station considered, the value of M_R is 1.15 and the Mach angle is 60°. It appears that the approximate results for the pressure field, comprised of many three-dimensional duct acoustic modes, in a gross sense represent disturbances propagating along the characteristic directions.

FIGURE B-2 BLADE ROW GEOMETRY AT RADIAL STATION $\sigma = 0.9$